

Supplementary Information - Biosynthetic reconstitution of deoxysugar phosphoramidate metalloprotease inhibitors using an N-P-bond-forming kinase

Alexandra Baulig, Irina Helmle, Marius Bader, Felix Wolf, Andreas Kulik, Arwa Al-Dilaimi, Daniel Wibberg, Jörn Kalinowski, Harald Gross, Leonard Kaysser*

*Correspondence to: leonard.kaysser@uni-tuebingen.de

Contents

Contents.....	1
Experimental Information.....	3
General methods	3
Analysis of compounds	3
Production and isolation conditions.....	3
Isolation of gDNA	3
Genome sequencing, assembly and annotation.....	3
Construction and screening of genomic libraries	4
Heterologous expression of the <i>tal</i> gene cluster	4
Cloning, expression and purification of <i>talE</i> /TalE.....	4
Production of cell-free protein extracts.....	4
Enzyme assay conditions for TalE and TalC.....	5
Isolation of 5	5
Gene inactivation	5
Tables	6
Table S1: NMR spectroscopic data of 4 in d_6 -DMSO (δ in ppm).	6
Table S2: NMR spectroscopic data of 5 in d_6 -DMSO (δ in ppm).	7
Table S3: PCR Primers.	8
Figures	9
Figure S1: UV-visible spectroscopic analysis.	9
Figure S2: HR-MS spectrum of 4.	10
Figure S3: HR-MS spectrum of 5.	11
Figure S4: HR-MS spectrum of 1 from host + <i>tal</i> cluster.....	12
Figure S5: MS analysis of 1 and 2.	13
Figure S6: MS analysis of the TalC assay.	14
Figure S7: LC-MS analysis of TalE and TalC assays.	15

Figure S8: MS/MS analysis of 4 and 5.	16
Figure S9: LC-MS analysis of the TalE assay with different enzyme concentrations.	17
Figure S10: SDS-Page TalE purification.	18
Figure S11: SDS-Page <i>talC</i> expression.	19
Figure S12: ¹ H NMR spectrum of 4 in <i>d</i> ₆ -DMSO (400 MHz).	20
Figure S13: ¹ H NMR spectrum of 4 in <i>d</i> ₆ -DMSO + H ₂ O (400 MHz).	21
Figure S14: ¹³ C NMR spectrum of 4 in <i>d</i> ₆ -DMSO (101 MHz).	22
Figure S15: DEPT135 NMR spectrum of 4 in <i>d</i> ₆ -DMSO (101 MHz).	23
Figure S16: ¹ H- ¹³ C multiplicity edited HSQC NMR spectrum of 4 in <i>d</i> ₆ -DMSO (400 MHz).	24
Figure S17: ¹ H- ¹ H COSY NMR spectrum of 4 in <i>d</i> ₆ -DMSO (400 MHz).	25
Figure S18: ¹ H- ¹³ C HMBC NMR spectrum of 4 in <i>d</i> ₆ -DMSO (400 MHz).	26
Figure S19: ¹ H- ¹³ C HSQC-TOCSY NMR spectrum of 4 in <i>d</i> ₆ -DMSO (400 MHz).	27
Figure S20: ¹ H- ¹ H NOESY NMR spectrum of 4 in <i>d</i> ₆ -DMSO (400 MHz).	28
Figure S21: ¹ H- ¹⁵ N HSQC NMR spectrum of 4 in <i>d</i> ₆ -DMSO (400 MHz).	29
Figure S22: ¹ H- ¹⁵ N HMBC NMR spectrum of 4 in <i>d</i> ₆ -DMSO (400 MHz).	30
Figure S23: ¹ H NMR spectrum of 5 in <i>d</i> ₆ -DMSO (400 MHz).	31
Figure S24: DEPT135 NMR spectrum of 5 in <i>d</i> ₆ -DMSO (101 MHz).	32
Figure S25: ¹ H- ¹³ C multiplicity edited HSQC NMR spectrum of 5 in <i>d</i> ₆ -DMSO (400 MHz).	33
Figure S26: ¹ H- ¹ H COSY NMR spectrum of 5 in <i>d</i> ₆ -DMSO (400 MHz).	34
Figure S27: ¹ H- ¹³ C HMBC NMR spectrum of 5 in <i>d</i> ₆ -DMSO (400 MHz).	35
Figure S28: ³¹ P NMR spectrum of 5 in <i>d</i> ₆ -DMSO (162 MHz).	36
Figure S29: δ _P -reference values of selected phosphoramidate-containing natural products and synthetic compounds.	37
Figure S30: ¹ H- ³¹ P HMBC NMR spectrum of 5 in <i>d</i> ₆ -DMSO (400 MHz).	38
Figure S31: Homologous phosphoramidate pathways.	39
References	40

Experimental Information

General methods

Chemicals, microbiological and molecular biological agents were purchased from standard commercial sources. The phosphoramidon standard and the synthetic L-Leu-L-Trp dipeptide were purchased from Sigma-Aldrich. *Streptomyces mozunensis* MK-23 (NRRL 12054) was obtained from the ARS Culture Collection, *Streptomyces* sp. MK730-62F2 (FERM BP-7218) was obtained from the National Institute of Advanced Industrial Science and Technology (AIST). The strains and their derivatives were grown and maintained on ISP-2 agar (0,4% yeast extract, 1% malt extract, 0,4% glucose, 2% agar; purchased from Becton Dickinson) or MS agar (2% soy flour, 2% mannitol, 2% agar; components purchased from Carl Roth). Liquid cultures of *Streptomyces mozunensis* MK-23 were cultivated in talopeptin production medium (10 g/L glycerol, 40 g/L peptone, 1 g/L K₂HPO₄, 1 g/L NaCl, 0.5 g/L MgSO₄ × 7H₂O, 0.01 g/L FeSO₄ × 7H₂O, 0.001 g/L ZnSO₄ × 7H₂O, 0.001 g/L CuSO₄ × 5H₂O and 0.001 g/L MnSO₄ × 6H₂O, pH 7). *Streptomyces* sp. MK730-62F2 and derivatives were cultivated in P1 production medium (10 g/L soytone, 10 g/L soluble starch, 20 g/L D-maltose, 5 mL/L trace element solution, pH 6.7) or Tryptic Soy Broth (TSB) medium (purchased from Becton Dickinson). Strains were stored as frozen spore suspensions in 20% glycerol at -80 °C. *Escherichia coli* strains were grown in LB medium (components purchased from Carl Roth) supplemented with appropriate antibiotics when required. DNA isolation and manipulations were carried out according to standard methods for *E. coli* and *Streptomyces*.^{1, 2} NMR solvents were obtained from Sigma-Aldrich.

Analysis of compounds

For the isolation of **5**, an Agilent 1100 HPLC system (Agilent 1100 series; Agilent Technologies) was used equipped with a Kinetex 5 μ XB-C18 100 Å 150 × 4.6 mm HPLC column. For LC-MS and MS/MS analysis of culture extracts, 2.5 μL of sample were injected onto a Nucleosil 100 C18 3 μm, 100 × 2 mm column fitted with a 10 × 2 mm precolumn at a flowrate of 0.4 mL/min and a linear gradient of t₀=0% solvent B (solvent B: acetonitrile (ACN) with 0.6% formic acid; solvent A: water with 0.1% formic acid) to t₁₅=100% B. The HPLC was coupled to a mass spectrometer with an electrospray ionization (ESI) interface (LC/MSD Ultra Trap System XCT 6330; Agilent 1200 series; Agilent Technologies). MS analysis was performed by ESI (positive and negative ionization) in Ultra Scan mode with a capillary voltage of 3.5 kV and drying gas temperature of 350 °C. High-resolution mass spectra were recorded on an HR-ESI-TOF-MS maXis 4G mass spectrometer (BRUKER DALTONIK GmbH, Bremen, Germany). 1D and 2D NMR spectra were acquired with an Avance III HD 400 MHz NMR spectrometer (Bruker BioSpin GmbH, Rheinstetten, Germany). NMR spectra were measured in d₆-DMSO at 293 K and were referenced to residual solvent signals (d₆-DMSO, δ_H=2.50 and δ_C=39.5 ppm) or the internal offset for ¹⁵N and ³¹P assigned by the instrument manufacturer (Bruker).

Production and isolation conditions

Production of phosphoramidon (**1**) was achieved by inoculating and cultivating 10 μL of spore suspension of *Streptomyces* sp. MK730-62F2 (mutants) in 50 mL of TSB broth at 30 °C and 200 rpm for 2 days. 1 mL of the cultures were transferred to 50 mL P1 production medium and cultivated at 30 °C at 200 rpm for 7 days. The whole cell culture was adjusted to pH 4 and one volume of butanol (BuOH) was added. The organic phase was collected and evaporated under reduced pressure. Resulting crude extracts were dissolved in 1 mL MeOH and then subjected to LC-MS and MS/MS analysis.

Production of talopeptin (**2**) was achieved by inoculating and cultivating 10 μL of spore suspension of *Streptomyces mozunensis* MK-23 (wildtype) in 50 mL talopeptin production medium³ at 30 °C and 200 rpm. After two days of cultivation, cultures (1 mL) were transferred to inoculate a mainculture of 50 mL talopeptin production medium in a 300 mL Erlenmeyer flask. After 3 days of cultivation at 30 °C and 200 rpm, the whole cell cultures were extracted with one volume of butanol (BuOH). The organic phase was isolated and evaporated to dryness under reduced pressure. Resulting crude extracts were dissolved in 1 mL MeOH and then subjected to LC-MS and MS/MS analysis.

Phosphoramidon (**1**) eluted after 7.5 min and talopeptin (**2**) after 7.7 min. For chemical complementation experiments, synthetic L-Leu-L-Trp dipeptide was added after 24 h of cultivation in a 5 mM final concentration.

Isolation of gDNA

To isolate genomic DNA of *Streptomyces mozunensis* MK-23 a 500 mL glycerol stock was used to inoculate 50 mL of TSB followed by cultivation at 30 °C and 200 rpm for 72 h. Cells were harvested and genomic DNA was isolated by phenol-chloroform extraction.²

Genome sequencing, assembly and annotation

Genomic DNA of *S. mozunensis* MK-23 was isolated as described by Kieser *et al.* and DNA quality was assessed by gel-electrophoresis. The quantity of DNA was estimated by a fluorescence-based method using the Quant-iT PicoGreen dsDNA kit (Invitrogen) and the Tecan Infinite 200 Microplate Reader (Tecan Deutschland GmbH). A whole-genome-shotgun PCRfree library (Nextera DNA Sample Prep Kit, Illumina) and an additional 8K mate pair library (Nextera Mate

Pair Sample Preparation Kit, Illumina) was generated according to the manufacturers protocol. Both sequencing libraries were sequenced on an Illumina MiSeq system (2 x 300 bases) at the Center for Biotechnology (CeBiTec), Bielefeld University. Upon sequencing and processing of the raw data, a *de novo* assembly was performed using the GS De Novo Assembler software release version 2.8 (Roche) with default settings. The *S. mozunensis* MK-23 draft genome consists of eight scaffolds with a total size of 8.744.153 bp containing 7708 protein coding genes with an overall GC content of 72.86%. Automatic gene predictions and annotation of coding sequences on the draft genome of *S. mozunensis* MK-23 was performed within the genome annotation systems Prokka v1.11⁴ and GenDB 2.0.⁵ The draft genome sequence was deposited in NCBI/EMBL-EBI/DDJB and is available under Bioproject number PRJEB30891.

Construction and screening of genomic libraries

Genomic DNA of *S. mozunensis* MK-23 was isolated as described above. For fosmid library construction, the gDNA was sheared by pipetting to yield approximately 40 kb fragments. Fragments were then cloned into the vector pCCFOS1 according to the manufacturers instructions to generate a genomic library containing 1920 clones. To isolate the *tal* biosynthetic gene cluster, the genomic library of *S. mozunensis* MK-23 was screened with the primer pairs talUS_FP/RP and talDS_FP/RP (Table S3) to identify the fosmid clone 8G9 containing a 39.446 bp insert. Restriction analysis and end-sequencing confirmed that fosmid 8G9 contains the complete *tal* cluster. *In silico* analysis was performed with BLAST⁶, antiSMASH⁷ and Artemis (Wellcome Trust Genome Campus; Cambridge; UK). The sequence of the *tal* cluster is available at NCBI under the accession number MK644118. Information on the *tal* gene cluster has also been deposited at the MIBiG database.⁸

Heterologous expression of the *tal* gene cluster

To allow stable chromosomal integration the chloramphenicol resistance gene *cat* in fosmid 8G9 was replaced by an integration cassette (*int_neo*) by λ -Red-mediated recombination to generate fosmid talMB01. The *int_neo* cassette contains an attachment site (*attP*) and the integrase gene (*int*) of phage Φ C31, a kanamycin resistance gene (*neo*) and an origin of transfer (*oriT*) to allow site-specific integration into most *Streptomyces* chromosomes.⁹ The cassette was obtained as an *Xba*I restriction fragment from merLK01, as described previously.¹⁰ The resulting fosmid talMB01 was verified by restriction analysis and transferred into *E. coli* ET12567.¹¹ Introduction in *Streptomyces* sp. MK730-62F2 was achieved by triparental intergeneric conjugation with the help of *E. coli* ET12567/pUB307.¹² Kanamycin resistant exconjugants, were selected and designated as *Streptomyces* sp. MK730-62F2/talMB01 (1-3). Production and extraction procedure of cultures of phosphoramidon (**1**) and LC-MS and MS/MS analysis was carried out as described above. The identity of **1** was further verified by HR-MS with measured *m/z* 542.19152 [M-H]⁻ (calcd for C₂₃H₃₃N₃O₁₀P, 542.19090, $\Delta=+1.13$ ppm) (Figure S4).

Cloning, expression and purification of *talE*/TalE

The gene *talE* was amplified from genomic DNA of *S. mozunensis* MK-23 using the primer pairs his_ talE_FP and his_ talE_RP (Table S3). The PCR product was cloned into pHis8 encoding for an N-terminal 8xHis-tag, yielding pHis8-*talE*, and was verified by restriction mapping and sequencing. pHis8-*talE* was transferred into *E. coli* Rosetta™ (DE3) pLysS by electroporation. A single colony was inoculated in 5 mL LB and cultivated at 37 °C at 200 rpm overnight. 100 mL TB medium was inoculated with 5 mL preculture and grown to an OD₆₀₀ of approximately 0.6. Expression of the recombinant proteins was induced by adding a final concentration of 500 mM Isopropyl β -D-1-thiogalactopyranoside (IPTG) and the culture was further cultivated over night at 20 °C at 220 rpm.

Cells were harvested and suspended in 4 mL lysis buffer (50 mM Tris-HCl, 500 mM NaCl, 10% glycerol, 10 mM β -mercaptoethanol, 20 mM imidazole, 0.5 mg/mL Lysozyme). Cell lysis was achieved by sonication for 10 min (ultrasonic disintegrator set to: amp 30%, 1 °C, pulse 5 s/5 s rest). Soluble and insoluble fractions were separated by centrifugation (4 °C, 18.000 rpm, 45 min). Soluble lysate was loaded onto a Ni-Agarose affinity column and washed twice with 4 mL wash buffer (lysis buffer without lysozyme). Recombinant protein was eluted with 2 mL elution buffer (wash buffer with 250 mM imidazole). Final protein concentration was quantified photometrically.

A discontinuous SDS-Page was carried out in a standard SDS-PAGE gel system (Bio-Rad). SDS-gels with a 4% and 12% polyacrylamide concentration were used as stacking and separating gel, respectively. Stacking was performed at 100 V, whereas separating was carried out at 160 V. SDS-Pages were stained with Coomassie Brilliant Blue R-250. Protein sizes were determined with Amersham low molecular weight marker (Figure S10).

Production of cell-free protein extracts

The production of TalC/TalE-containing cell-free extracts were achieved by inoculating and cultivating 10 μ L of spore suspension of *Streptomyces* sp. MK730-62F2 (Δ talC/ Δ talE mutants) in 50 mL of TSB broth supplemented with appropriate antibiotics at 30 °C and 200 rpm for 2 days. 1 mL of the precultures were transferred to 100 mL P1 production medium and cultivated at 30 °C at 200 rpm for 3 days. After incubation, the cultures were hold on ice, harvested by centrifugation (5.000 \times g, 10 min), suspended in 2.5 mL per gram of cells in Tris-HCl buffer, supplemented with 1 mg/mL Lysozyme. Cells

were disrupted by sonication as described above. The cell-free protein extracts were stored on -20 °C until used for further enzyme assays.

Enzyme assay conditions for TalE and TalC

Standard TalE enzyme assay contained 50 mM Tris-HCl pH 7.5, 5 mM Mg²⁺, 1 mM ATP, 2.5 mM dipeptide and 10 μM TalE in a total of 50 μL reaction volume. The assay was performed at 30 °C for 2 h and stopped by the addition of 100 μL methanol. For the TalC assay, 5 mM dTDP-L-rhamnose and a TalC-containing cell-free extract were added to a running TalE assay after 2 hours and incubated for another 16 h at 30 °C. The reaction was stored on -20 °C until subjected to LC-MS, MS/MS and HR-MS analysis, NMR or purification. Negative controls did not contain ATP, enzyme (TalE), dTDP-L-rhamnose or TalC (protein extract of *ΔtalC* mutant).

Isolation of **5**

For the isolation of **5**, an enzyme assay with TalE was conducted as described above up-scaled to a total volume of 10 mL. Separation of **5** was performed on a reversed phase HPLC column (Kinetex 5μ XB-C18 100 Å 150 x 4.6 mm; 280 nm detection; with a flowrate of 1 mL/min and a linear gradient from t₀=10% solvent B to t₇=100% solvent B (solvent B: acetonitrile (ACN) with 0.06% formic acid; solvent A: water with 0.1% formic acid). **5** eluted after 4.9 min, was collected and dried under reduced pressure to give 4.37 mg as white powder. LC-MS and MS/MS analysis of **5** was performed on a reversed phase HPLC column (Agilent Eclipse Plus C18, 3.5 μm, 2.1 x 150 mm) by linear gradient elution from t₀=0% solvent B (solvent B: acetonitrile (ACN) with 0.6% formic acid; solvent A: water with 0.1% formic acid) to t₁₅=100% B at a flowrate of 0.4 mL/min. MS data were acquired in negative and positive mode. **5** eluted after 8.4 min. ¹H and ¹³C NMR spectroscopic data (Table S2); HR-MS: *m/z* 396.13400 [M-H]⁻ (calcd for C₁₇H₂₃N₃O₆P, 396.13300, Δ=+2.53 ppm) (Figure S3).

Gene inactivation

For gene deletion studies, a PCR targeting system was employed.¹³ An apramycin resistance cassette [*aac(3)IV*] was amplified from the plasmid pIJ773 with the primer pair *Δorf-7-orf-1_FP/RP* for the inactivation of *orf-7-orf-1*, primer pair *ΔtalC_FP/RP* for the inactivation of *talC*, primer pair *ΔtalD_FP/RP* for the inactivation of *talD*, primer pair *ΔtalE_FP/RP* for the inactivation of *talE* and primer pair *Δorf+1-orf+12_FP/RP* for the inactivation of *orf+1-orf+12* (Table S3). The ORFs and genes, respectively, were transferred into *E. coli* BW25113/pKD46 containing talMB01. The genes *orf-7-orf-1*, *talC*, *talD*, *talE* and *orf+1-orf+12* were replaced individually by the generated apramycin resistance cassettes with the help of λ-Red-mediated recombination.¹⁴ The resulting mutant fosmids talAB01 (*Δorf-7-orf-1*), fosmids talAB02 (*ΔtalC*), talAB03 (*ΔtalD*), talAB04 (*ΔtalE*) and talAB05 (*Δorf+1-orf+12*) were confirmed by restriction analysis. To generate precisely tailored in-frame mutations, the resistance cassettes were removed in *E. coli* BT340, taking advantage of the flanking Flp/FRT recognition site. Positive fosmids were screened for their apramycin sensitivity and verified by restriction analysis, PCR and sequencing of PCR products (Table S3). The fosmids were transferred into *E. coli* ET12567 as described above and introduced into *Streptomyces* sp. MK730-62F2, was accessed by triparental intergeneric conjugation with the help of *E. coli* ET12567/pUB307. Of the resulting mutant strains *Streptomyces* sp. MK730-62F2 *Δorf-7-orf-1*, *ΔtalC*, *ΔtalD*, *ΔtalE* and *Δorf+1-orf+12*, three clones per knock-out were further verified by PCR and tested for **1** production by LC-MS and MS/MS analysis.

Tables

Table S1: NMR spectroscopic data of 4 in d_6 -DMSO (δ in ppm).

residue	position	$\delta_{C/N}^a$	δ_H (protons, J in Hz) ^b	COSY	HMBC ^c
L-Leu	α	50.7 CH	3.76 (1, dd, 6.0, 6.0)	α -NH, β	β , γ , α -CO _{Leu}
	β	40.3 CH ₂	1.55 (2, m)	α , γ	α , γ , δ , ϵ , α -CO _{Leu}
	γ	23.4 CH	1.68 (1, m)	β , δ , ϵ	α , β , δ , ϵ
	δ	21.7 CH ₃	0.88 (3, d, 6.7)	γ	β , γ , ϵ
	ϵ	22.9 CH ₃	0.90 (3, d, 6.8)	γ	β , γ , δ
	α -CO _{Leu}	169.3 C _q			
	α -NH _{Leu}	38.8 ^d NH ₂	8.1 ^d (2, br s)	α	
L-Trp	α	53.2 CH	4.54 (1, ddd, 8.1, 7.6, 5.2)	α -NH, β	β , 3, α -CO _{Leu} , α -CO _{Trp}
	β_a β_b	27.0 CH ₂	3.09 (1, dd, 14.7, 8.1) 3.20 (1, dd, 14.7, 5.2)	α	α , 2, 3, 3a, α -CO _{Trp}
	NH-1	131.8 NH	10.91 (1, br s)	2	2, 3, 3a, 7a
	2	123.8 CH	7.19 (1, d, 2.3)	NH-1	β , 3, 3a, 7a
	3	109.4 C _q			
	3a	127.1 C _q			
	4	118.1 CH	7.55 (1, d, 7.9)	5	3, 3a, 6, 7, 7a
	5	118.4 CH	6.99 (1, m)	4, 6	3a, 7
	6	121.0 CH	7.07 (1, m)	5, 7	4, 7a
	7	111.4 CH	7.35 (1, dt, 8.1, 0.8)	6	3a, 5
	7a	136.1 C _q			
	α -CO _{Trp}	172.8 C _q			
α -NH _{Trp}	121.6 NH	8.80 (1, d, 7.6)	α	α , β , α -CO _{Leu}	

^a Recorded at 101 MHz for ¹³C and ¹⁵N NMR values were extracted from the corresponding ¹H-¹⁵N HMBC NMR spectrum. Multiplicity determined by an edited ¹H-¹³C HSQC and a DEPT135 NMR experiment. ^b Recorded at 400 MHz. ^c Protons showing long-range correlation with indicated carbon. ^d Only visible upon addition of minute volumes of H₂O.

Table S2: NMR spectroscopic data of 5 in d_6 -DMSO (δ in ppm).

residue	position	$\delta_{C/P}$ ^a	δ_H (protons, J in Hz) ^b	COSY	HMBC ^c
phosphate	P	-0.25 P			
L-Leu	α	52.0 CH	3.30 ^d	β	P
	β_a β_b	42.7 CH ₂	1.23 (1, m) 1.42 (1, m)	α, γ	
	γ	23.6 CH	1.66 (1, m)	β, δ, ϵ	
	δ	21.4 CH ₃	0.83 (3, d, 6.5)	γ	β, γ, ϵ
	ϵ	23.0 CH ₃	0.86 (3, d, 6.5)	γ	β, γ, δ
	α -CO _{Leu}	n.o. ^e			
	α -NH _{Leu}	n.o. ^e	n.o. ^e		
L-Trp	α	52.9 CH	4.42 (1, br s)	β	
	β_a β_b	27.1 CH ₂	3.07 (1, dd, 14.6, 7.3) 3.17 (1, dd, 14.6, 5.6)	α	$\alpha, 2, 3, 3a, \alpha$ -CO _{Trp}
	NH-1	n.o. ^e	10.83 (1, br s)		
	2	123.3 CH	7.11 (1, d, 1.7)		3, 3a, 7a
	3	109.9 ^f C _q			
	3a	127.4 ^f C _q			
	4	118.1 CH	7.52 (1, d, 7.6)	5	3, 6, 7a
	5	118.0 CH	6.95 (1, t, 7.6, 7.3)	4, 6	3a, 7
	6	120.5 CH	7.05 (1, t, 7.9, 7.3)	5, 7	4, 7a
	7	111.0 CH	7.31 (1, d, 7.9)	6	3a, 5
	7a	136.0 ^f C _q			
	α -CO _{Trp}	173.5 ^f C _q			
	α -NH _{Trp}	n.o. ^e	n.o. ^e		

^a Recorded at 101 MHz for ¹³C and at 162 MHz for ³¹P, respectively. Multiplicity determined by an edited ¹H-¹³C HSQC and a DEPT135 NMR experiment. ^b Recorded at 400 MHz. ^c Protons showing long-range correlation with indicated carbon or phosphate atom, respectively. ^d ¹H NMR value was extracted from ¹H-¹H COSY NMR spectrum. Coupling and integral not determinable due to overlap with H₂O resonance. ^e Not observable. ^f ¹³C NMR value was extracted from ¹H-¹³C HMBC NMR spectrum.

Table S3: PCR Primers.

Primer name	Primer sequence 5'→3'
<i>Δorf-1</i> _FP ^a	<i>TCCCGCCGAACGAGCCGGCACAGAGCCTGTCCGGCCCTAATCCGGGGATCCGTCGACC</i>
<i>Δorf-7</i> _RP ^a	<i>CGGACACGGGCGGAGGAGGCCGGCCTCGCTGGCCGAGTCATGTAGGCTGGAGCTGCTTC</i>
<i>ΔtalC</i> _FP ^a	<i>CTGATCCCCCATCCCCGAGTAAACGAGGTTCTTCATGATCCGGGGATCCGTCGACC</i>
<i>ΔtalC</i> _RP ^a	<i>CGCACCGTGTTTCGAGAACCGATGAGGCCGGGCCGGCCTCATGTAGGCTGGAGCTGCTTC</i>
<i>ΔtalD</i> _FP ^a	<i>CACGGGCCGAGTGAACCTTCCTTCAGGAGAAAACACGTTGATTCCGGGGATCCGTCGACC</i>
<i>ΔtalD</i> _RP ^a	<i>GCATGAAGGAACCTCGTTTACTCGGGATGGGGGGGATCATGTAGGCTGGAGCTGCTTC</i>
<i>ΔtalE</i> _FP ^a	<i>ATCGTGACATGATGACGAATGGCTGAACTGTGCGCATGATCCGGGGATCCGTCGACC</i>
<i>ΔtalE</i> _RP ^a	<i>GCGATGTGCGACCCGGCTGGTGCCACTCAGCCGGTGTGTCATGTAGGCTGGAGCTGCTTC</i>
<i>Δorf+1</i> _FP ^a	<i>GTAGGTCCCCGTACCGACACCGAAAGGACCTCCCCGTGATCCGGGGATCCGTCGACC</i>
<i>Δorf+12</i> _RP ^a	<i>CGGCGCGGCCTCCTCCCCGGCAGCTCGGAGCACGACATTGTAGGCTGGAGCTGCTTC</i>
<i>his_talE</i> _FP ^b	<i>CCGAATTCATGACCCGTTCCGGATCGC</i>
<i>his_talE</i> _RP ^b	<i>GGTGCTCGAGTACCCGGCGGTGCGG</i>
<i>talUS</i> _FP	<i>TCGATGCAACGCAGAGTTTC</i>
<i>talUS</i> _RP	<i>CTGTAGTCGGAGCAGGTGAG</i>
<i>talDS</i> _FP	<i>GCTGCCCTGTCGTACCTTTC</i>
<i>talDS</i> _RP	<i>GCTGGATGACGTGGGTCAAC</i>
<i>screenΔorf-1</i> _FP	<i>CGCAGCGGGACGAGATGACC</i>
<i>screenΔorf-7</i> _RP	<i>CGGGTGTGCGGGTGAGACAG</i>
<i>screenΔtalC</i> _FP	<i>CCGGATCGCGCAACTGGCTC</i>
<i>screenΔtalC</i> _RP	<i>ACAGGAGCACGCCGGGTACG</i>
<i>screenΔtalD</i> _FP	<i>TCGCCCCGACGAGAGCTACGC</i>
<i>screenΔtalD</i> _RP	<i>TCTCGACCACCCGCCGCATC</i>
<i>screenΔtalE</i> _FP	<i>CGATGGCGTGATCCGTCGGG</i>
<i>screenΔtalE</i> _RP	<i>GCGGGAAGGCGTACTCCAGC</i>
<i>screenΔorf+1</i> _FP	<i>GTCACCGGCAACACCGCAGG</i>
<i>screenΔorf+12</i> _RP	<i>GGGTCGCACCATCGGGACTC</i>

^a Italicized letters allow homologous recombination via PCR targeted mutagenesis.

^b Overlapping regions with pHis8.

Figures

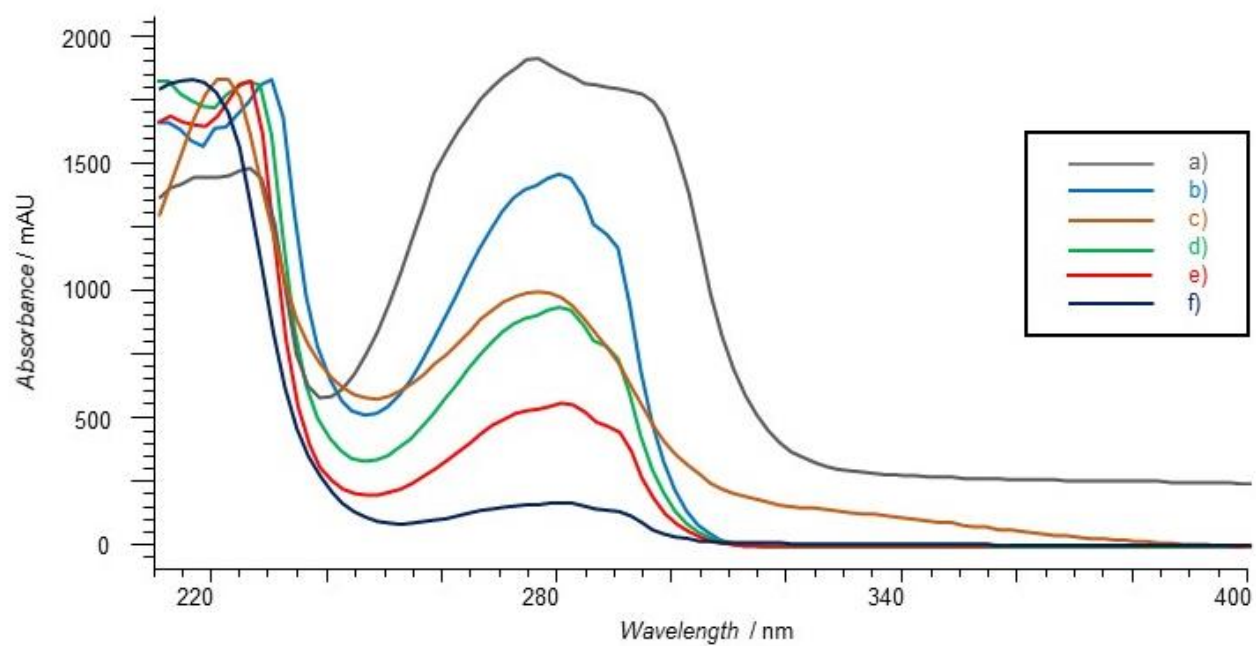


Figure S1: UV-visible spectroscopic analysis.

a) *S. mozunensis* (**2**; t_R 7.7 min) b) standard of **1** (t_R 7.5 min) c) host + *tal* cluster (**1**; t_R 7.5 min) d) dipeptide standard (**4**) e) TalE assay product (**5**) and f) TalC assay product (**1**).

Display Report

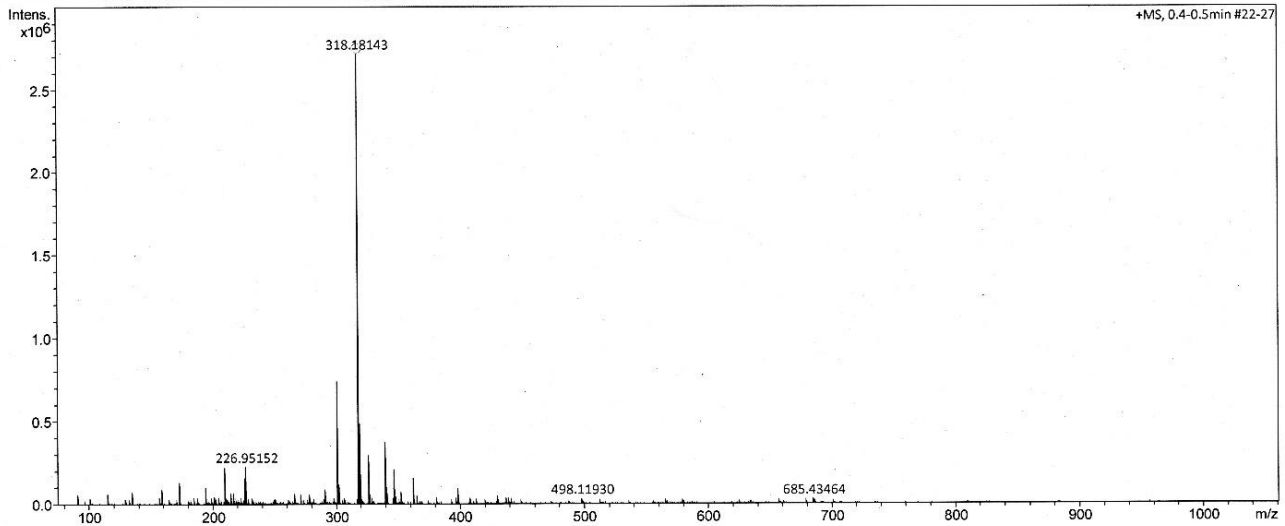
Analysis Info

Analysis Name D:\Data\oi\Kaysser_Baulig_Nr1_181018_GE6_01_27398.d
Method fia_ms_80-1000l_pos_neu.m
Sample Name Kaysser_Baulig_Nr1_181018
Comment

Acquisition Date 10/18/2018 11:28:21 AM
Operator BDAL@DE
Instrument maXis 288882.21253

Acquisition Parameter

Source Type	ESI	Ion Polarity	Positive	Set Nebulizer	1.2 Bar
Focus	Active	Set Capillary	4500 V	Set Dry Heater	200 °C
Scan Begin	80 m/z	Set End Plate Offset	-500 V	Set Dry Gas	6.0 l/min
Scan End	1050 m/z	Set Charging Voltage	0 V	Set Divert Valve	Waste
		Set Corona	0 nA	Set APCI Heater	0 °C



Kaysser_Baulig_Nr1_181018_GE6_01_27398.d
Bruker Compass DataAnalysis 4.2

printed: 10/23/2018 4:06:31 PM

by: BDAL@DE

Page 1 of 1

Figure S2: HR-MS spectrum of 4.

HR-ESI-TOF-MS [M+H]⁺ m/z 318.18143 (calcd for C₁₇H₂₄N₃O₃, 318.18122, Δ=+0.66 ppm).

Display Report

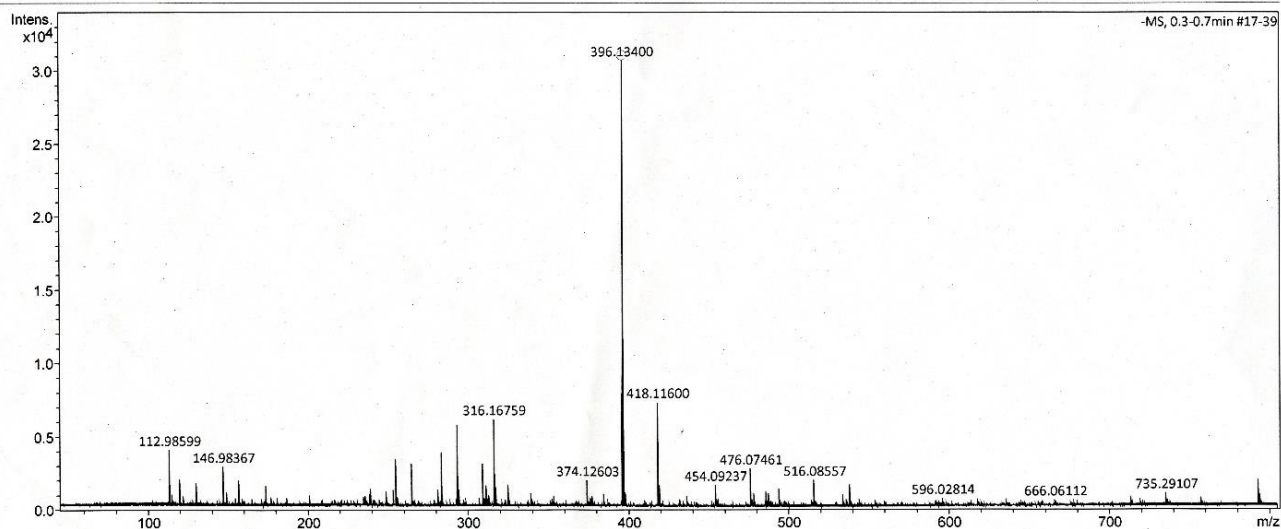
Analysis Info

Analysis Name D:\Data\oi\Kaysser_Baulig_Nr2_181018_GE7_01_27413.d
Method fia_ms_50-800_neg_neu.m
Sample Name Kaysser_Baulig_Nr2_181018
Comment

Acquisition Date 10/18/2018 5:52:24 PM
Operator BDAL@DE
Instrument maXis 288882.21253

Acquisition Parameter

Source Type	ESI	Ion Polarity	Negative	Set Nebulizer	1.2 Bar
Focus	Not active	Set Capillary	4500 V	Set Dry Heater	200 °C
Scan Begin	50 m/z	Set End Plate Offset	-500 V	Set Dry Gas	6.0 l/min
Scan End	800 m/z	Set Charging Voltage	0 V	Set Divert Valve	Waste
		Set Corona	0 nA	Set APCI Heater	0 °C



Kaysser_Baulig_Nr 2_181018_GE7_01_27413.d
Bruker Compass DataAnalysis 4.2

printed: 10/23/2018 6:26:23 PM

by: BDAL@DE

Page 1 of 1

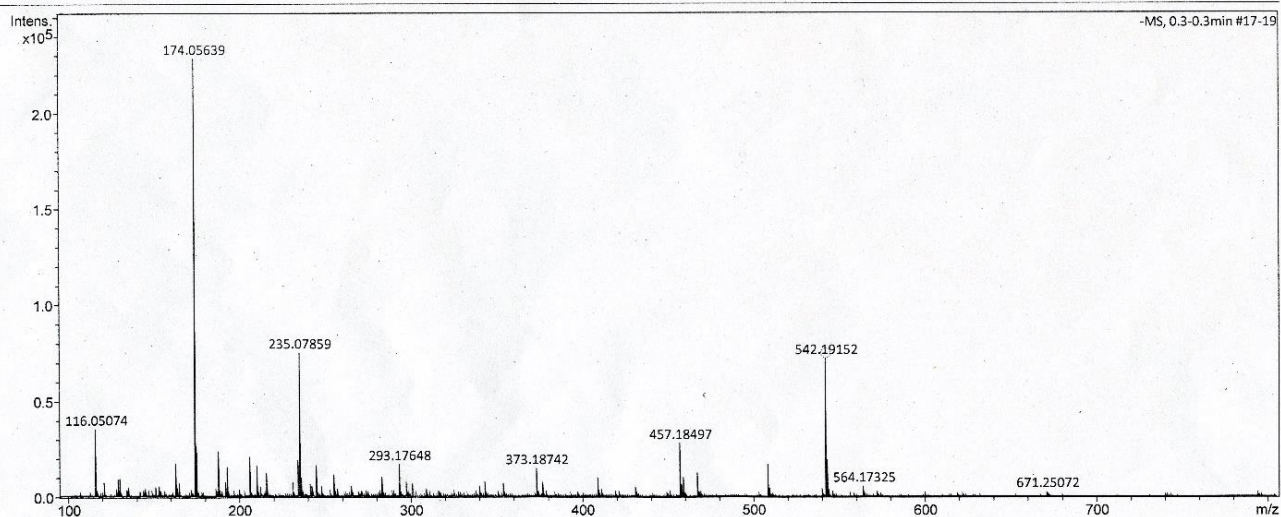
Figure S3: HR-MS spectrum of 5.

HR-ESI-TOF-MS [M-H]⁻ m/z 396.13400 (calcd for C₁₇H₂₃N₃O₆P, 396.13300, Δ=+2.53 ppm).

Display Report

Analysis Info
Analysis Name: D:\Data\oi\Bader_CPZ_Peak4_GC6_01_11943.d
Method: fia_ms_100-800_neg_neu.m
Sample Name: Bader_CPZ_Peak4
Comment:
Acquisition Date: 9/22/2016 3:46:56 PM
Operator: BDAL@DE
Instrument: maXis 288882.21253

Acquisition Parameter
Source Type: ESI
Focus: Not active
Scan Begin: 100 m/z
Scan End: 800 m/z
Ion Polarity: Negative
Set Capillary: 4000 V
Set End Plate Offset: -500 V
Set Charging Voltage: 0 V
Set Corona: 0 nA
Set Nebulizer: 1.2 Bar
Set Dry Heater: 200 °C
Set Dry Gas: 6.0 l/min
Set Divert Valve: Waste
Set APCI Heater: 0 °C



Bader_CPZ_Peak4_GC6_01_11943.d
Bruker Compass DataAnalysis 4.2

printed: 10/5/2016 5:31:18 PM

by: BDAL@DE

Page 1 of 1

Figure S4: HR-MS spectrum of 1 from host + tal cluster.

HR-ESI-TOF-MS [M-H]⁻ m/z 542.19152 (calcd for C₂₃H₃₃N₃O₁₀P, 542.19090, Δ=+1.13 ppm).

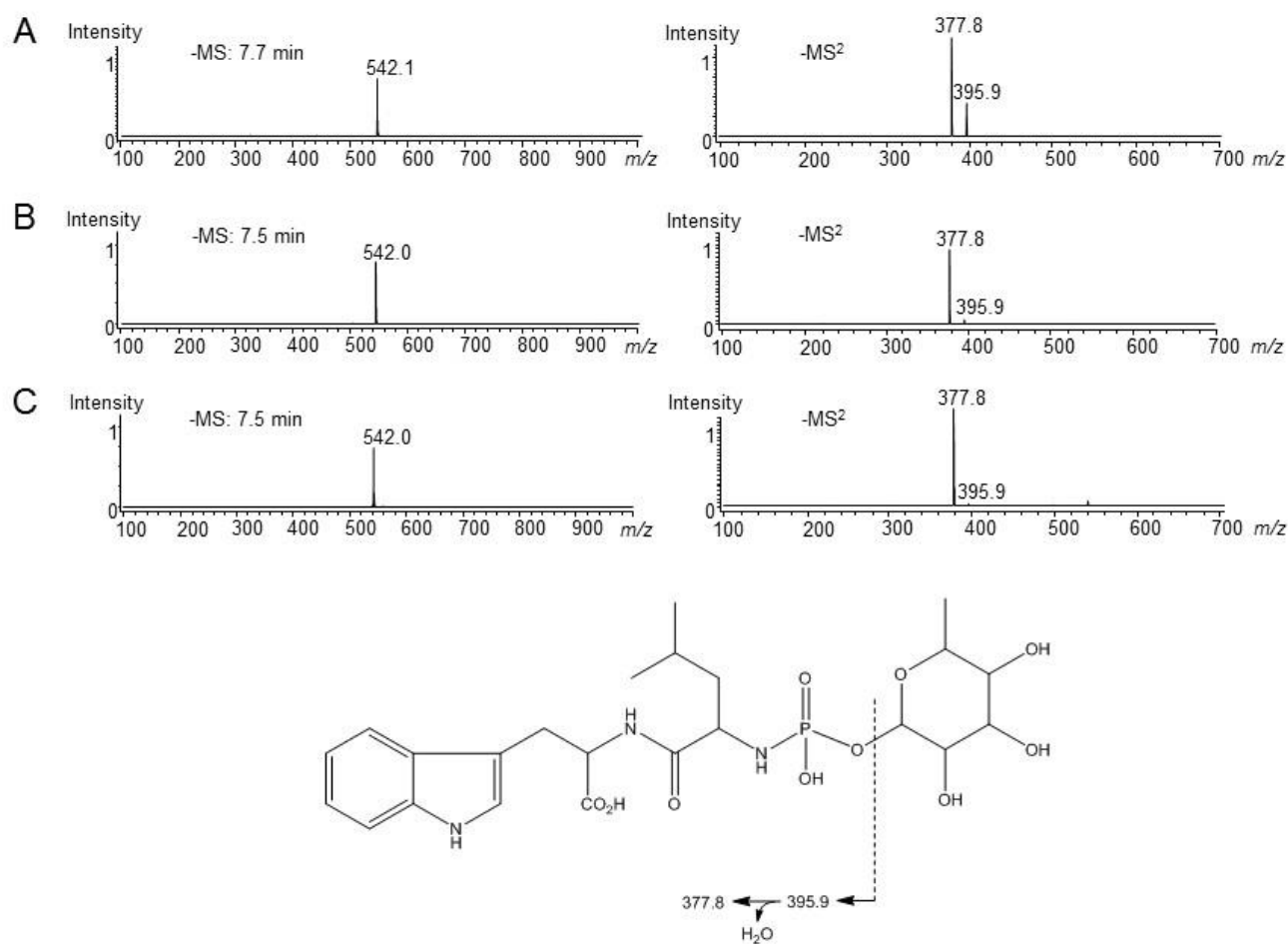


Figure S5: MS analysis of 1 and 2.

Negative mode MS spectra (left) and MS/MS spectra (right) from LC analysis of (A) **2** in *S. mozunensis*, (B) **1** standard, (C) **1** in host + *tal* cluster and a proposed fragmentation scheme of compound **1** and **2**.¹⁵

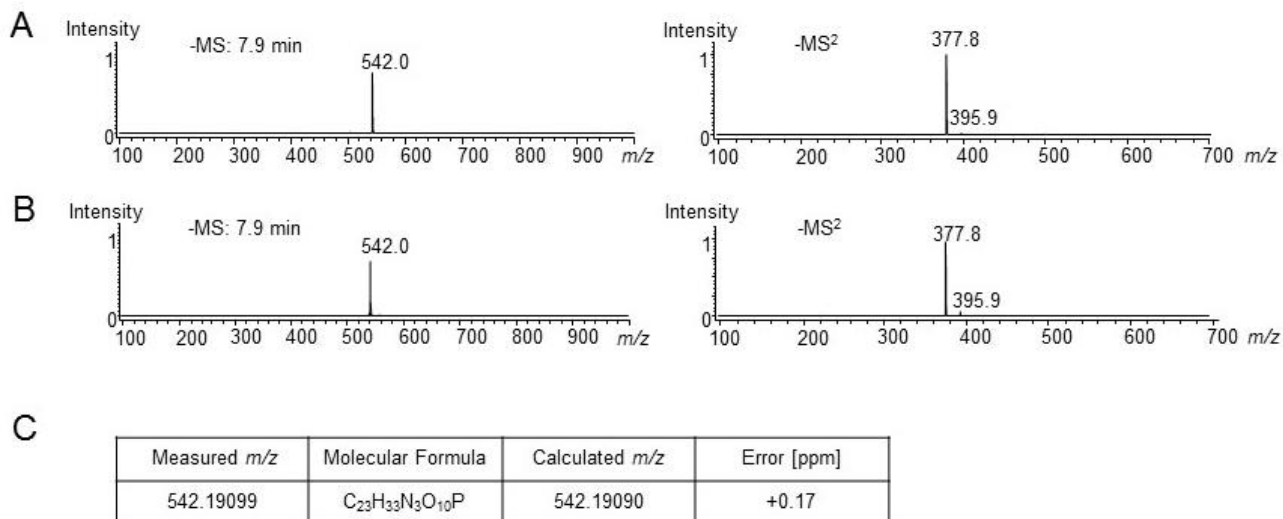


Figure S6: MS analysis of the TalC assay.

Negative mode MS spectra (left) and MS/MS spectra (right) from LC analysis of (A) standard and (B) TalC assay product (1). (C) HR-MS measurements of the TalC product peak.

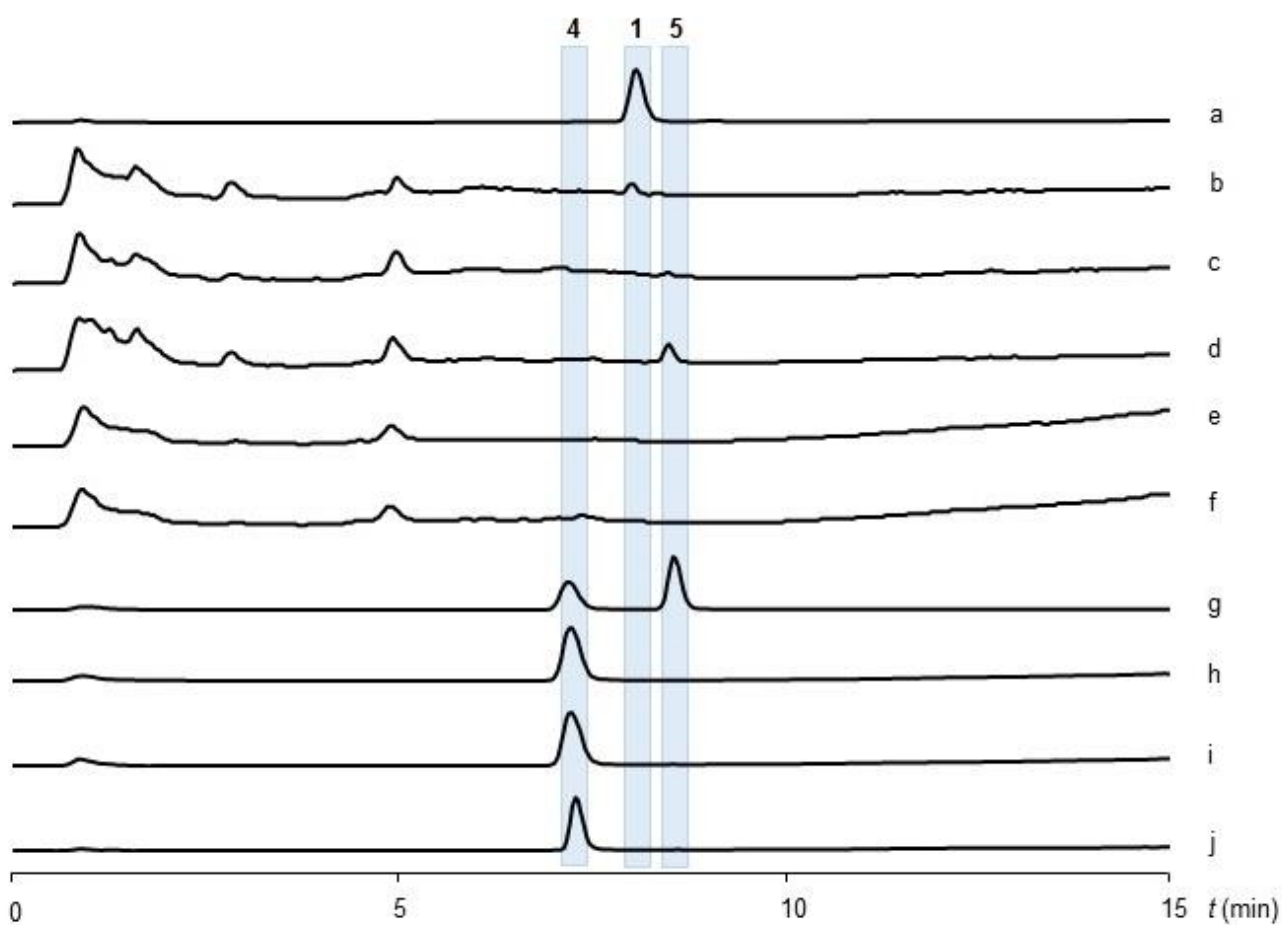


Figure S7: LC-MS analysis of TalE and TalC assays.

Total ion current-chromatograms (TICs). a) Commercial standard of **1**. b) Enzymatic assay with TalC (protein extract of $\Delta talE$ mutant), dTDP-L-rhamnose, TalE, **4** and ATP. c) Control assay of b) without TalC using a protein extract of the $\Delta talC$ mutant. d) Control assay of b) without dTDP-L-rhamnose. e) Control assay without TalC (protein extract of $\Delta talC$ mutant) with **4**. f) Control assay TalC (protein extract of $\Delta talE$ mutant) with **4**. g) Enzymatic assay of TalE with **4** and ATP. h) Control assay of g) without TalE. i) Control assay of g) without ATP. j) Control assay of g) without **4**.

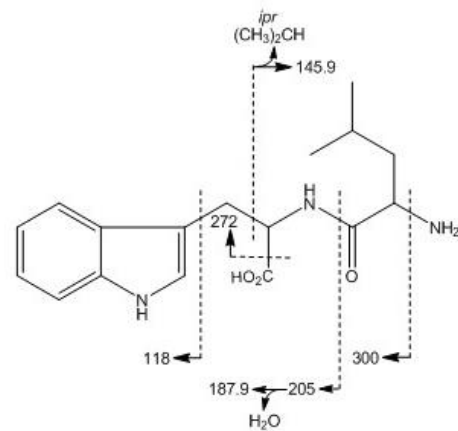
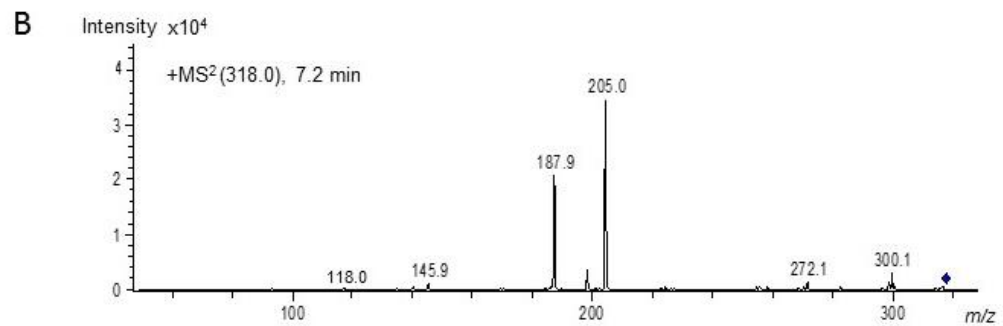
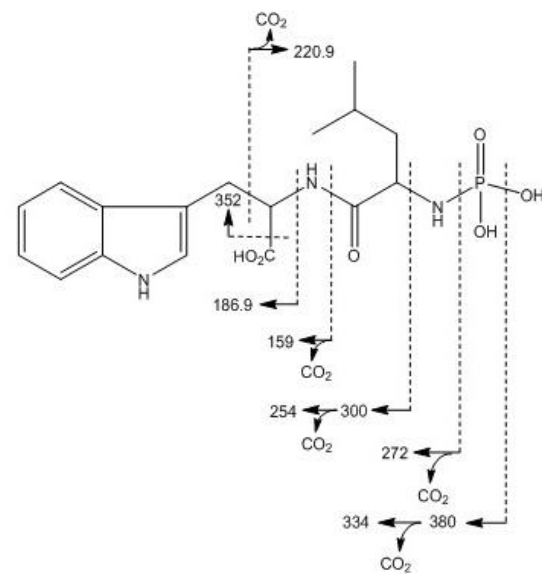
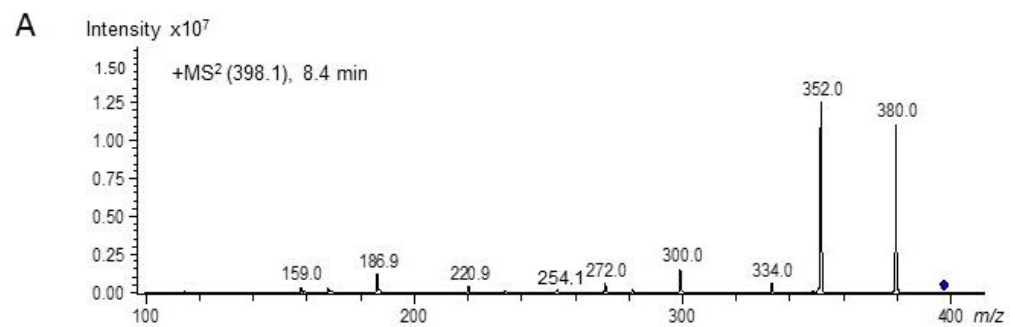


Figure S8: MS/MS analysis of 4 and 5.

MS/MS spectra and proposed fragmentation scheme of (A) **5** and (B) **4** in positive mode. Fragmentation schemes were predicted by MetFrag.¹⁶

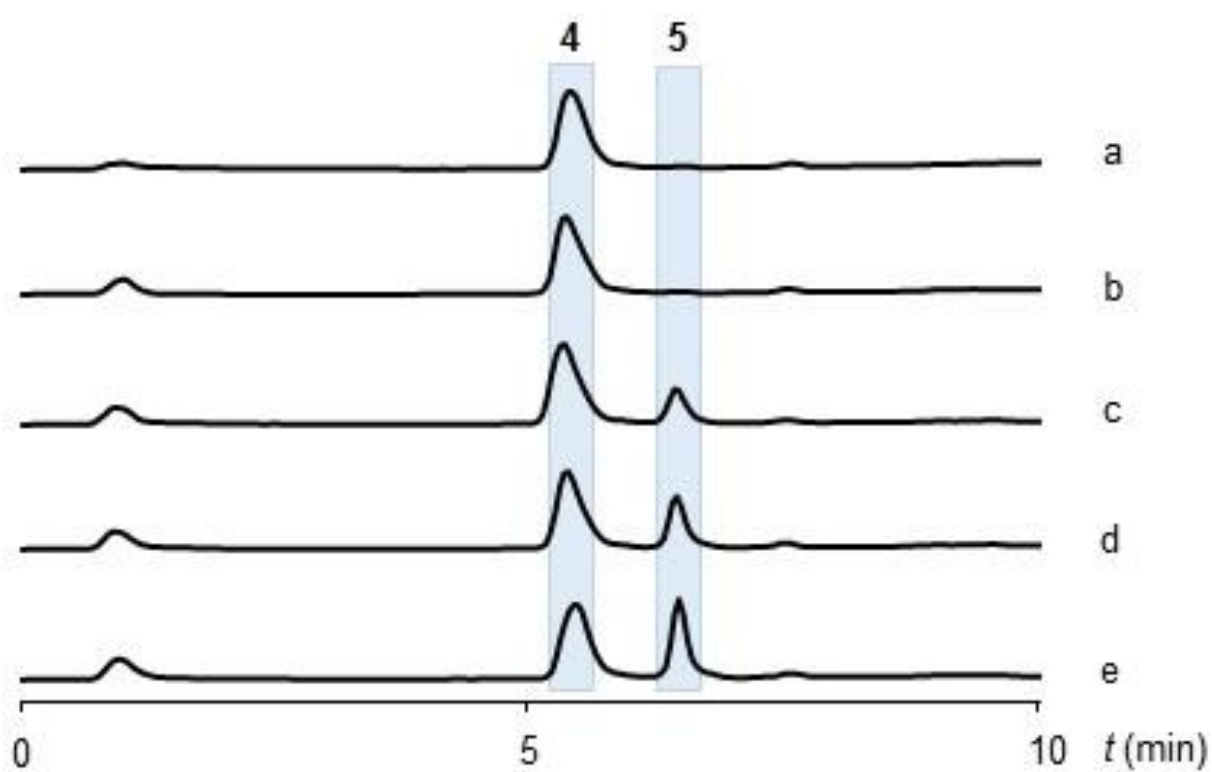


Figure S9: LC-MS analysis of the TalE assay with different enzyme concentrations.

LC-MS analysis was carried out as described above using a modified linear gradient of $t_0=10\%$ solvent B (solvent B: acetonitrile (ACN) with 0.6% formic acid; solvent A: water with 0.1% formic acid) to $t_{15}=100\%$ B.

Total ion current-chromatograms (TICs) of a) Control assay with 4 and ATP without TalE. b) Assay with $2.5 \mu\text{M}$ TalE. c) Assay with $5 \mu\text{M}$ TalE. d) Assay with $7.5 \mu\text{M}$ TalE. e) Assay with $10 \mu\text{M}$ TalE.

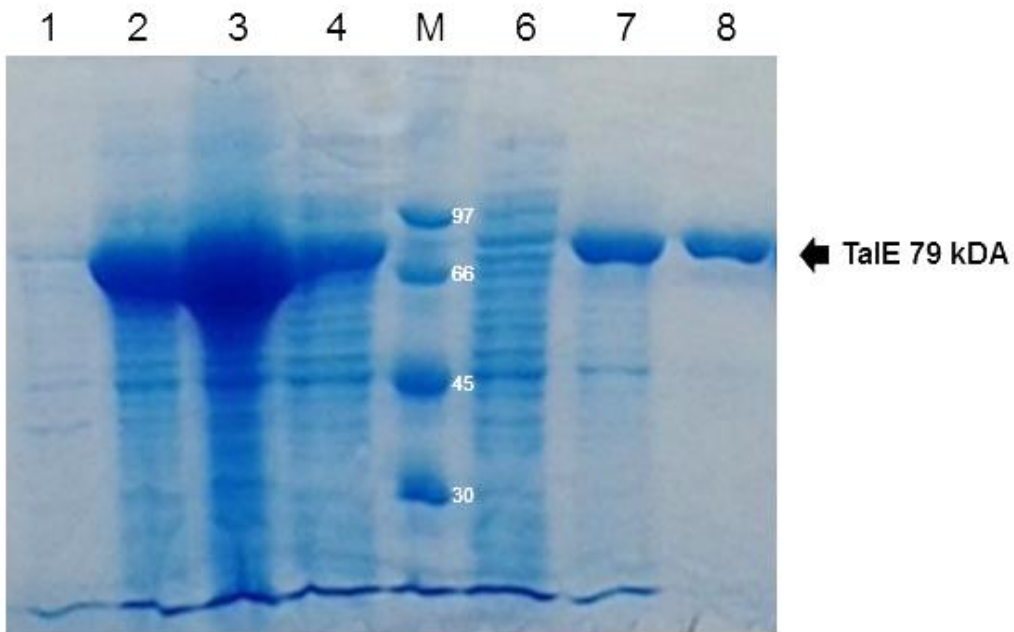


Figure S10: SDS-Page TaIE purification.

Coomassie stained SDS-page, showing the expression and purification of TaIE. Marker (M) indicates protein size in kDa. Lane 1 shows whole cell lysate before induction, lane 2 shows whole cell lysate after induction. An approximately 79 kDa band appears after induction, as expected for TaIE. Lane 3 represents cell pellet after lysis and lane 4 the supernatant after lysis. Lane 6 shows the flow-through and lane 7 the wash after Ni-NTA. Lane 8 shows the eluted protein of 79 kDa after Ni-NTA chromatography.

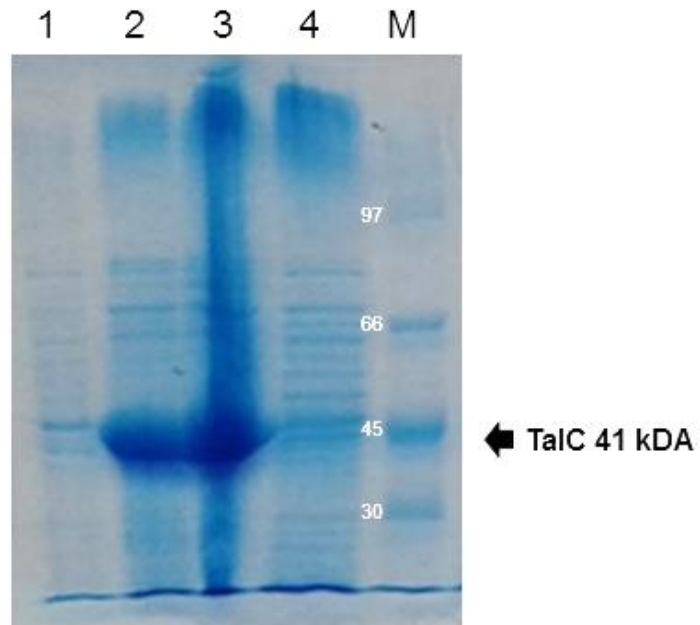


Figure S11: SDS-Page *talC* expression.

Coomassie stained SDS-page, showing expression of *talC*. Marker (M) indicates protein size in kDa. Lane 1 shows whole cell lysate before induction, lane 2 shows whole cell lysate after induction. An approximately 41 kDa band appears after induction, as expected for TalC. Lane 3 represents the cell pellet after lysis containing insoluble TalC, and lane 4 shows the supernatant after lysis with no visible band for TalC.

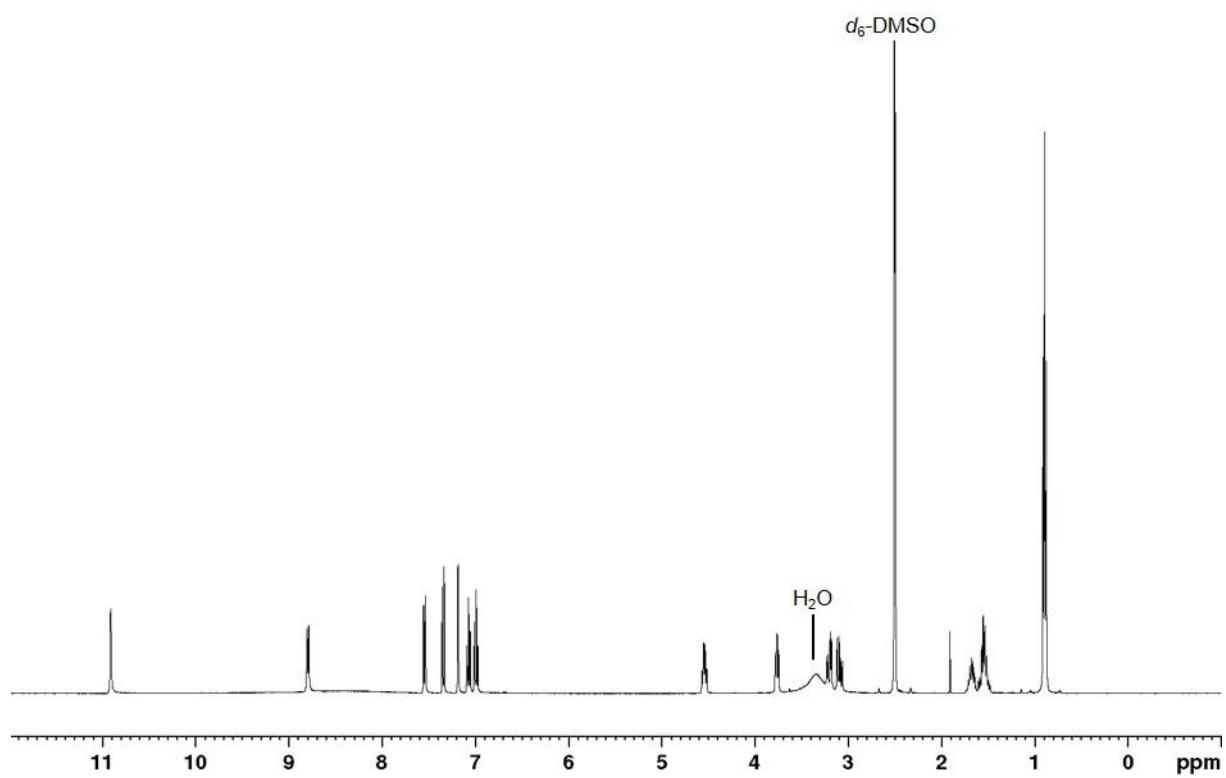


Figure S12: ^1H NMR spectrum of 4 in d_6 -DMSO (400 MHz).

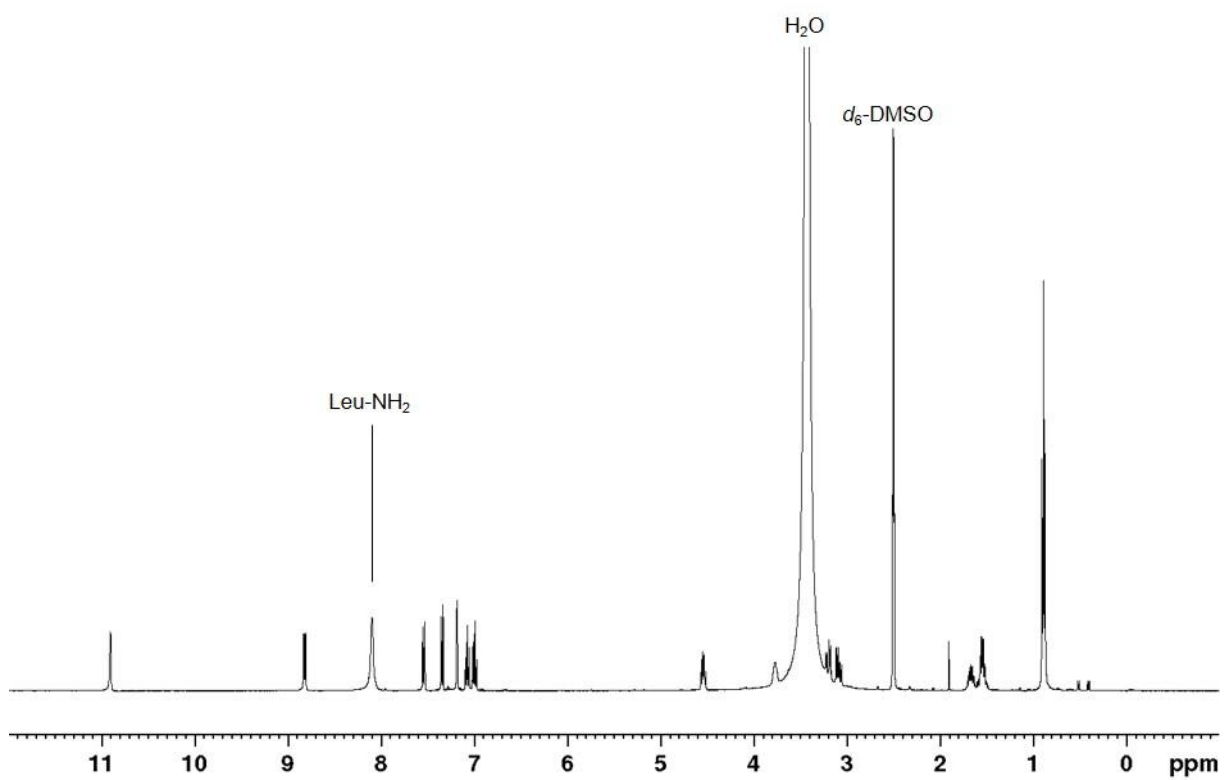


Figure S13: ^1H NMR spectrum of **4** in d_6 -DMSO + H_2O (400 MHz).

Addition of H_2O enabled the detection of Leu-NH₂.

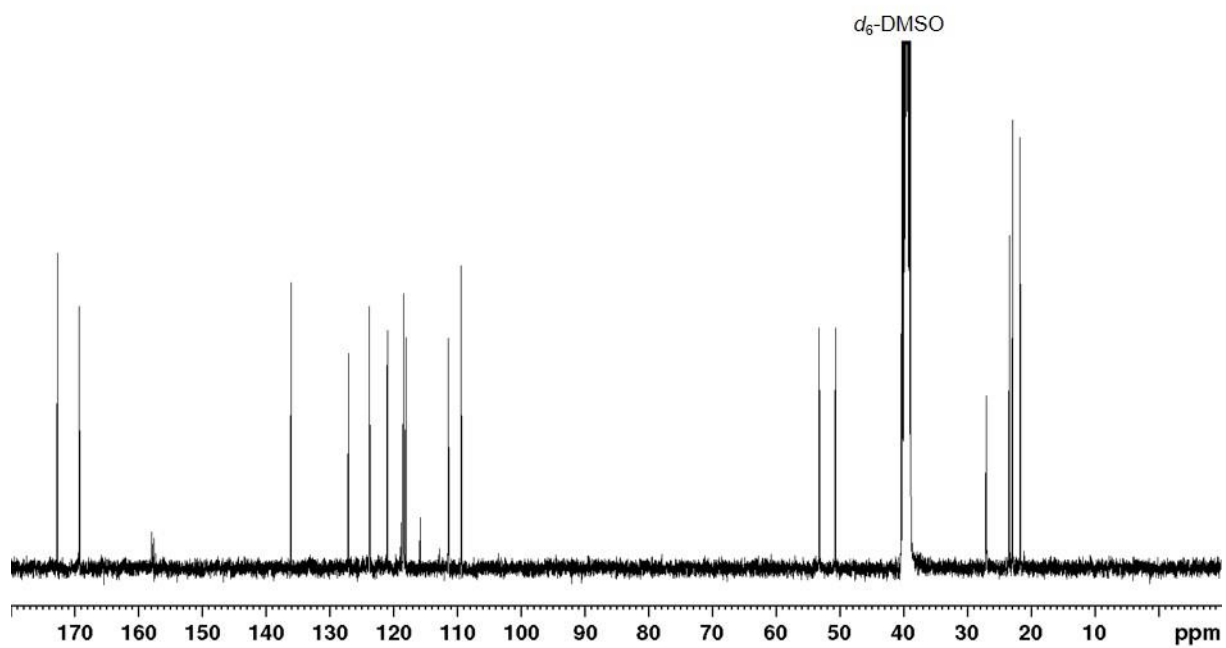


Figure S14: ^{13}C NMR spectrum of 4 in d_6 -DMSO (101 MHz).

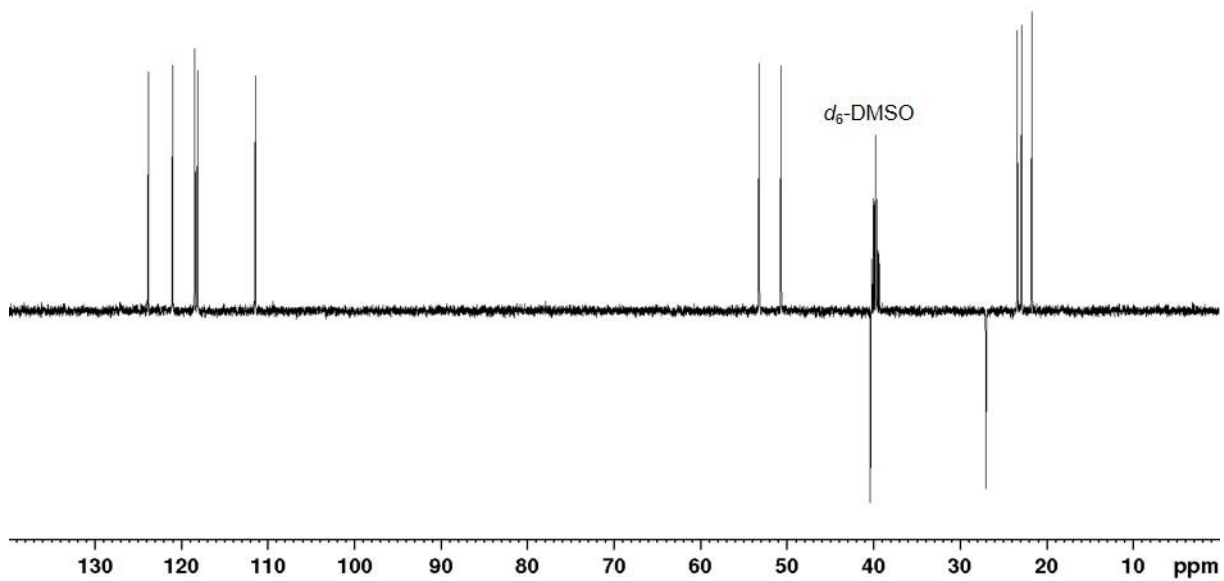


Figure S15: DEPT135 NMR spectrum of 4 in d_6 -DMSO (101 MHz).

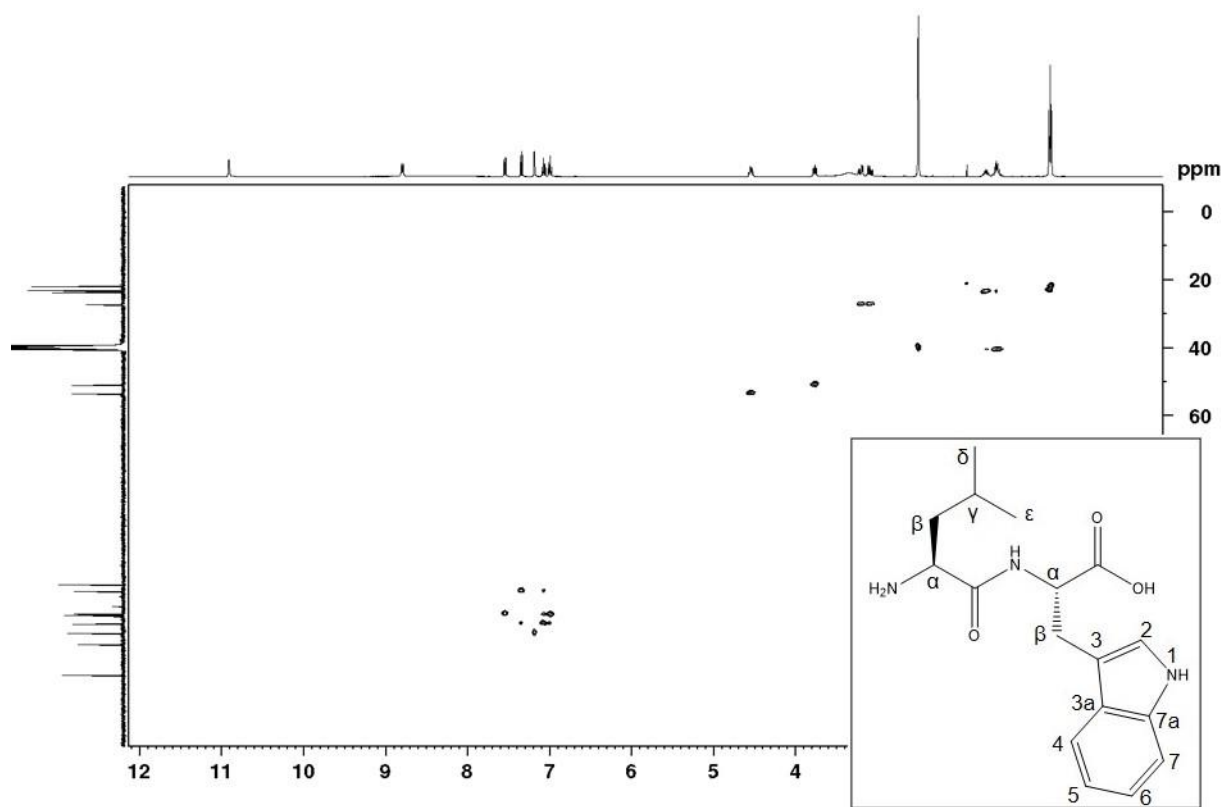


Figure S16: ^1H - ^{13}C multiplicity edited HSQC NMR spectrum of 4 in d_6 -DMSO (400 MHz).

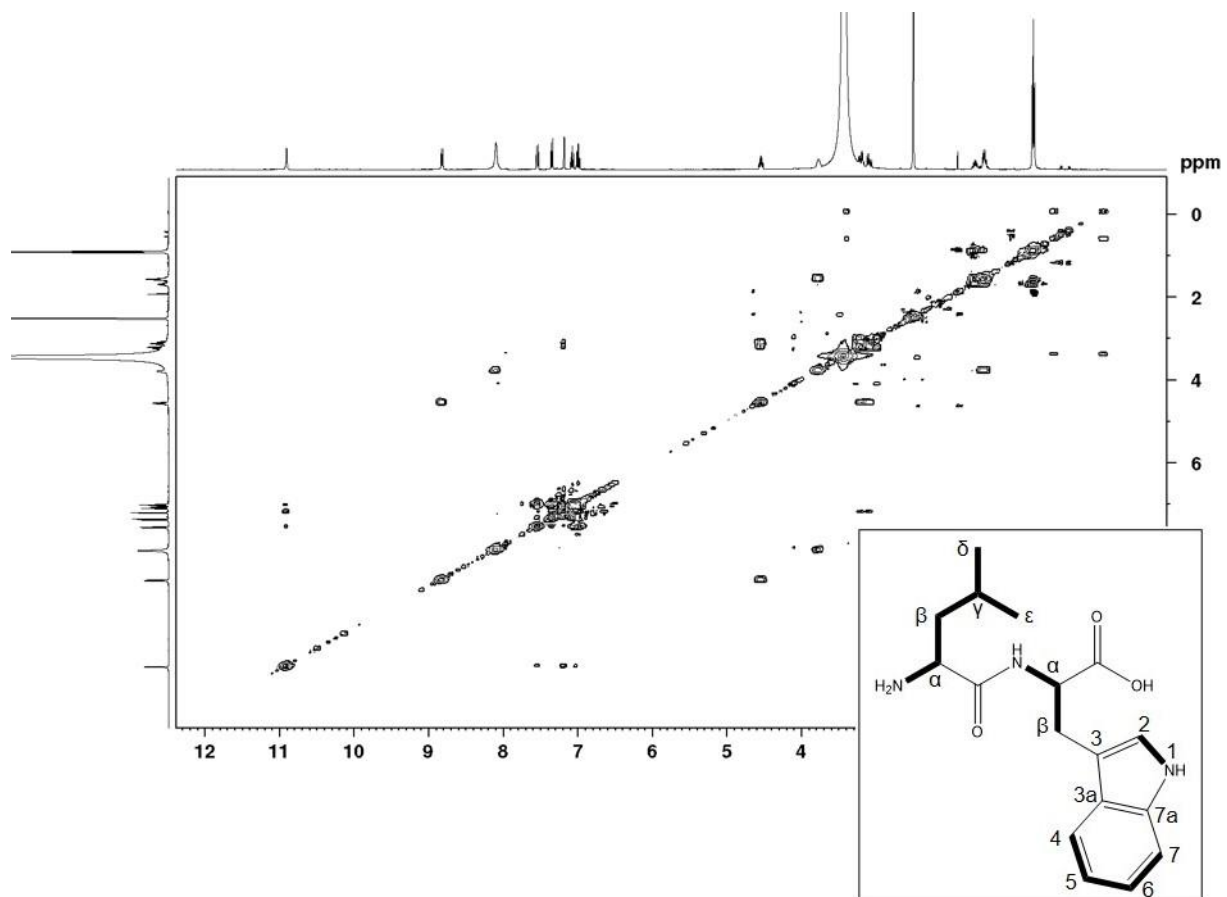


Figure S17: ^1H - ^1H COSY NMR spectrum of **4** in d_6 -DMSO (400 MHz).

Bold lines in the insert represent the observed ^1H - ^1H COSY correlations.

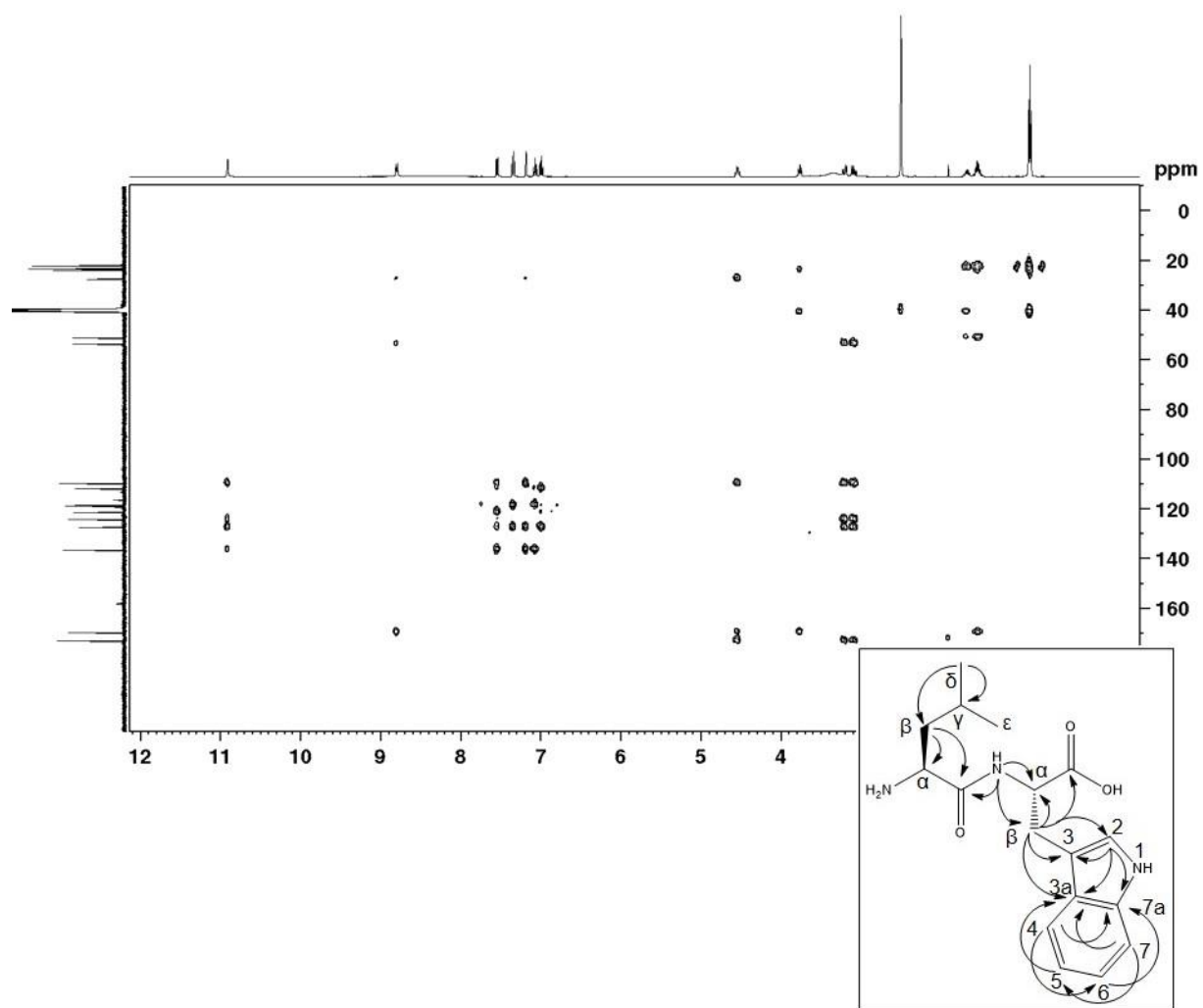


Figure S18: ^1H - ^{13}C HMBC NMR spectrum of 4 in d_6 -DMSO (400 MHz).

Arrows indicate key ^1H - ^{13}C HMBC long-range correlations.

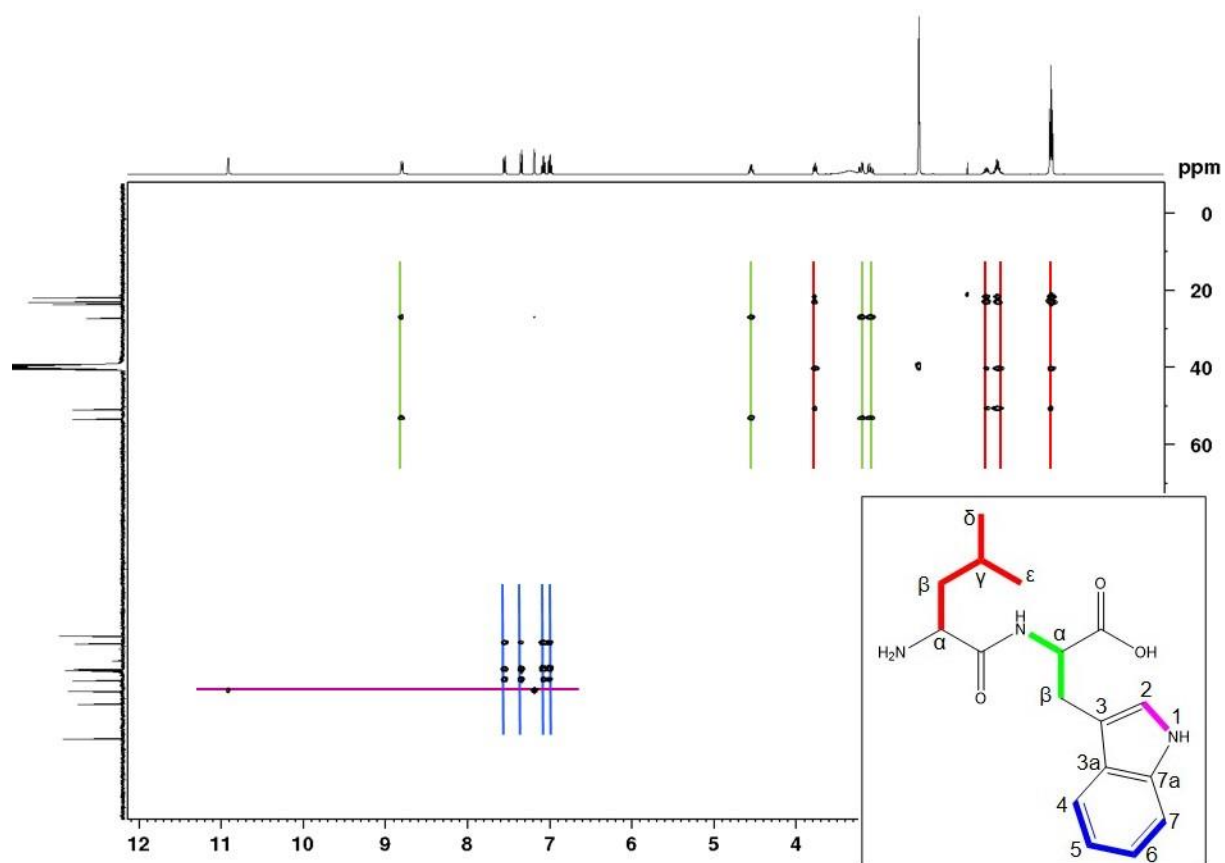


Figure S19: ^1H - ^{13}C HSQC-TOCSY NMR spectrum of 4 in d_6 -DMSO (400 MHz).

The four spin systems are marked in red, green, purple and blue.

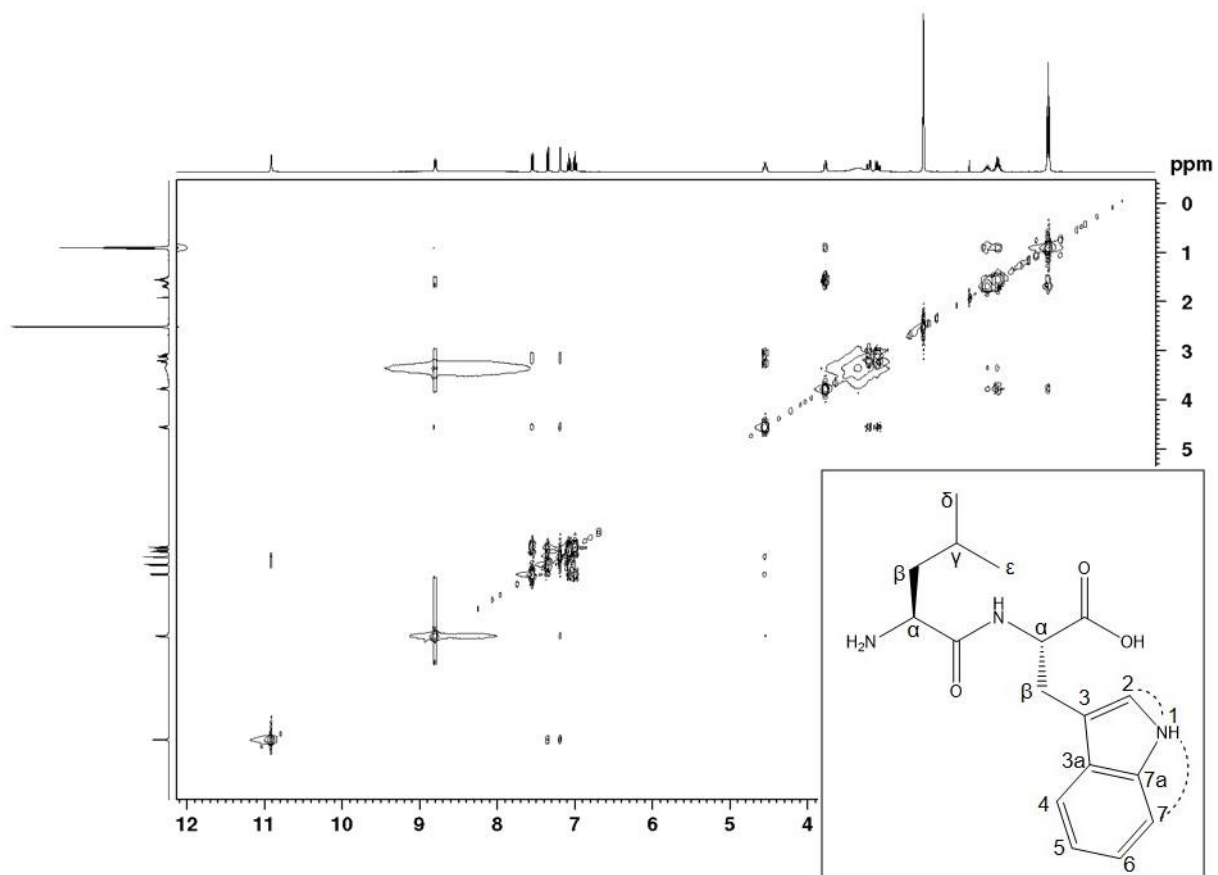


Figure S20: ^1H - ^1H NOESY NMR spectrum of 4 in d_6 -DMSO (400 MHz).
Dashed lines indicate the ^1H - ^1H NOESY through space key correlations.

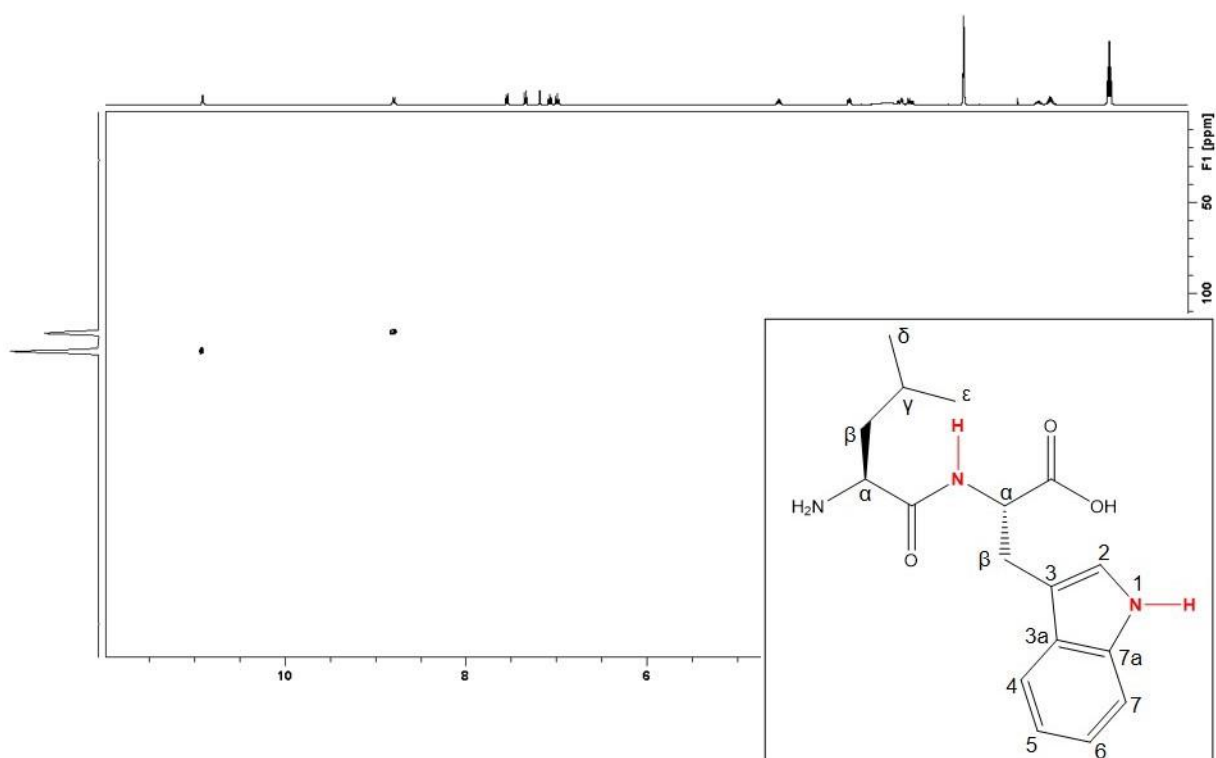


Figure S21: ^1H - ^{15}N HSQC NMR spectrum of **4** in d_6 -DMSO (400 MHz).

Red lines indicate the observed ^1H - ^{15}N HSQC correlations.

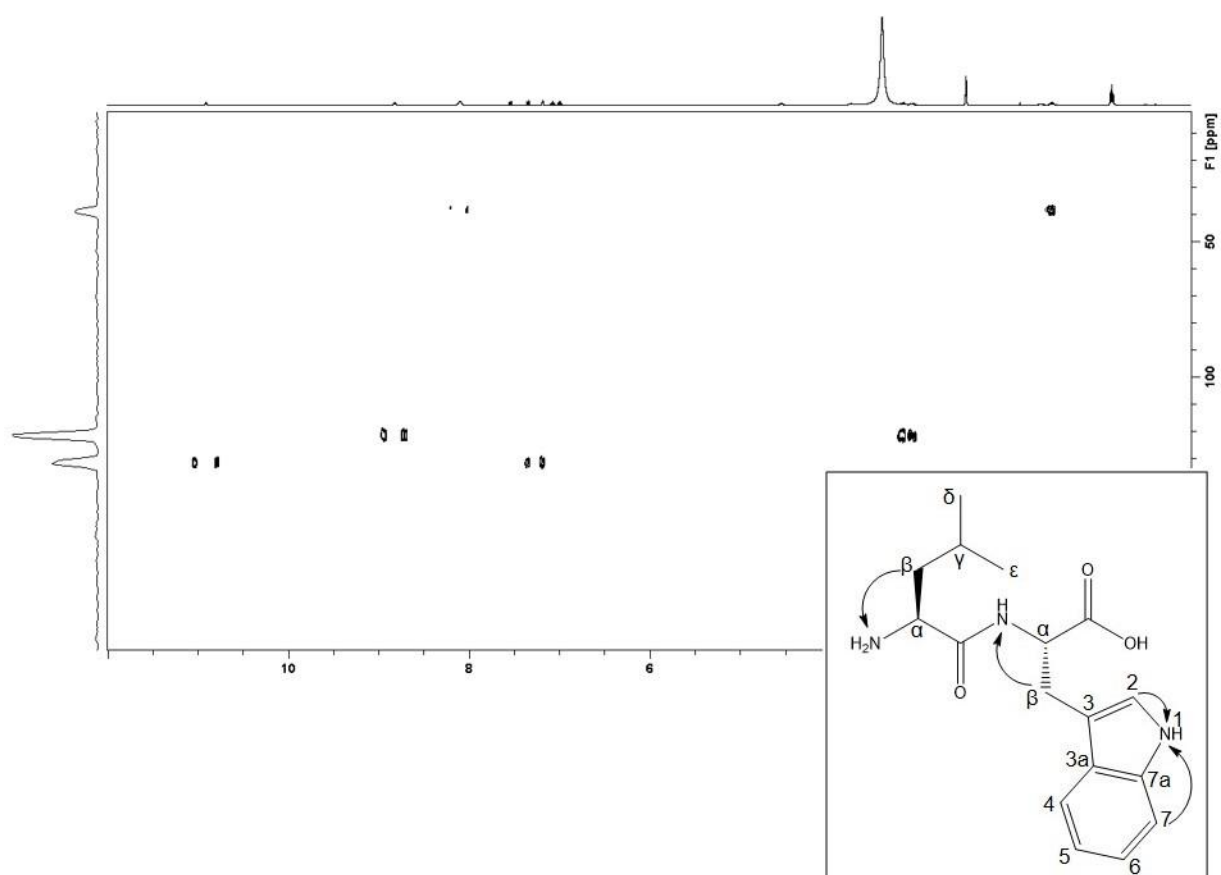


Figure S22: ^1H - ^{15}N HMBC NMR spectrum of **4** in d_6 -DMSO (400 MHz).

Arrows indicate key ^1H - ^{15}N HMBC long-range correlations.

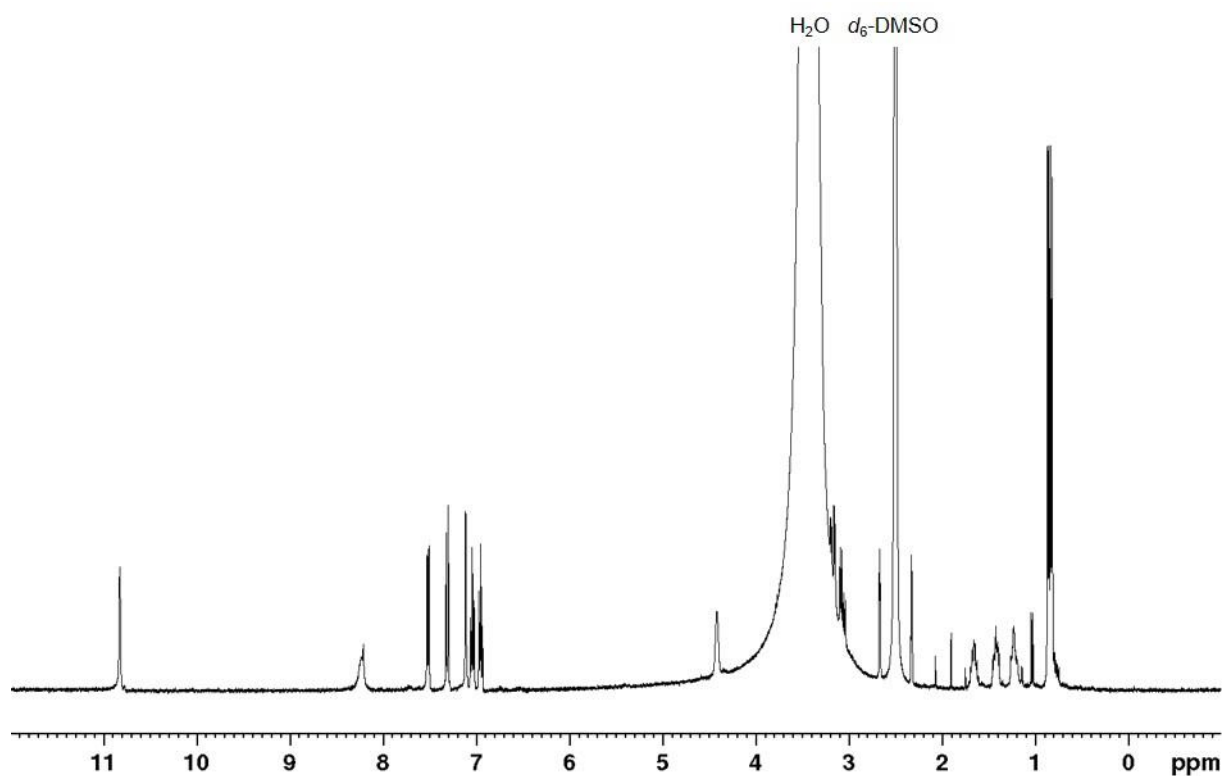


Figure S23: ^1H NMR spectrum of 5 in d_6 -DMSO (400 MHz).

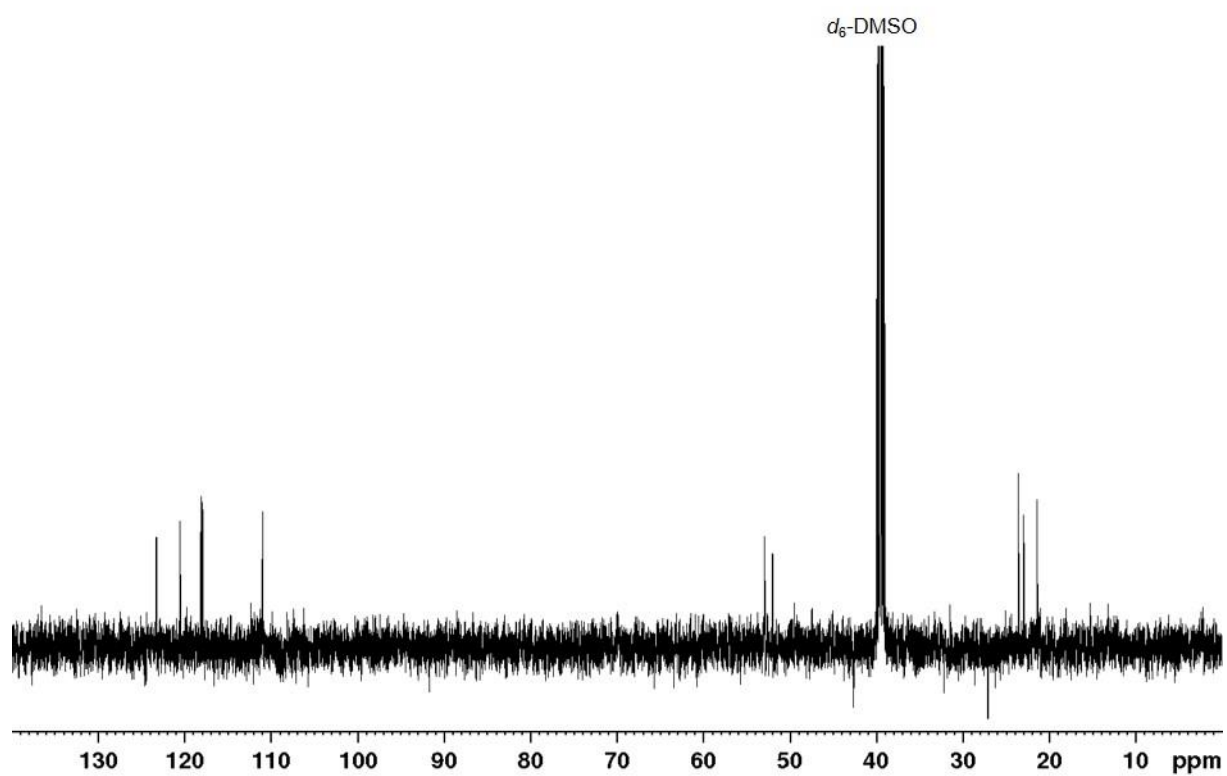


Figure S24: DEPT135 NMR spectrum of 5 in *d*₆-DMSO (101 MHz).

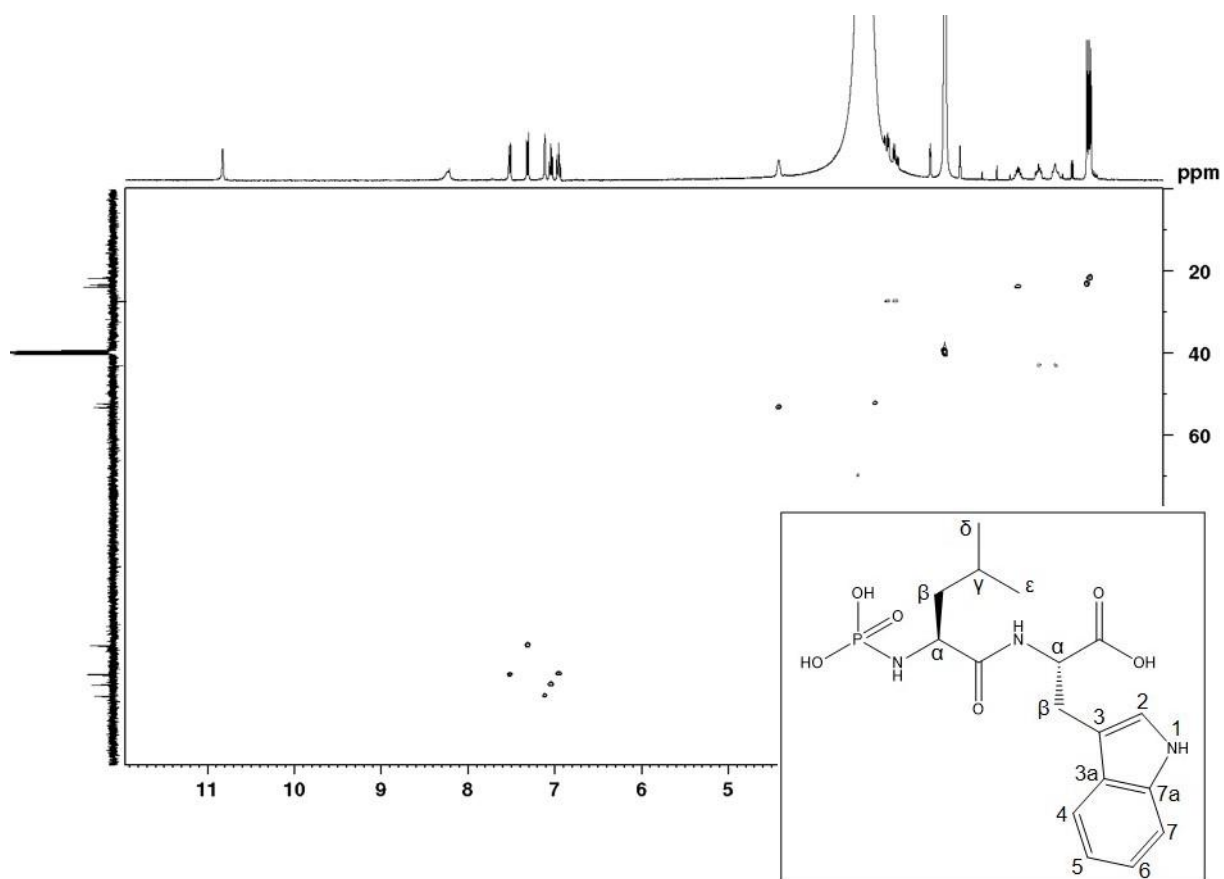


Figure S25: ^1H - ^{13}C multiplicity edited HSQC NMR spectrum of 5 in d_6 -DMSO (400 MHz).

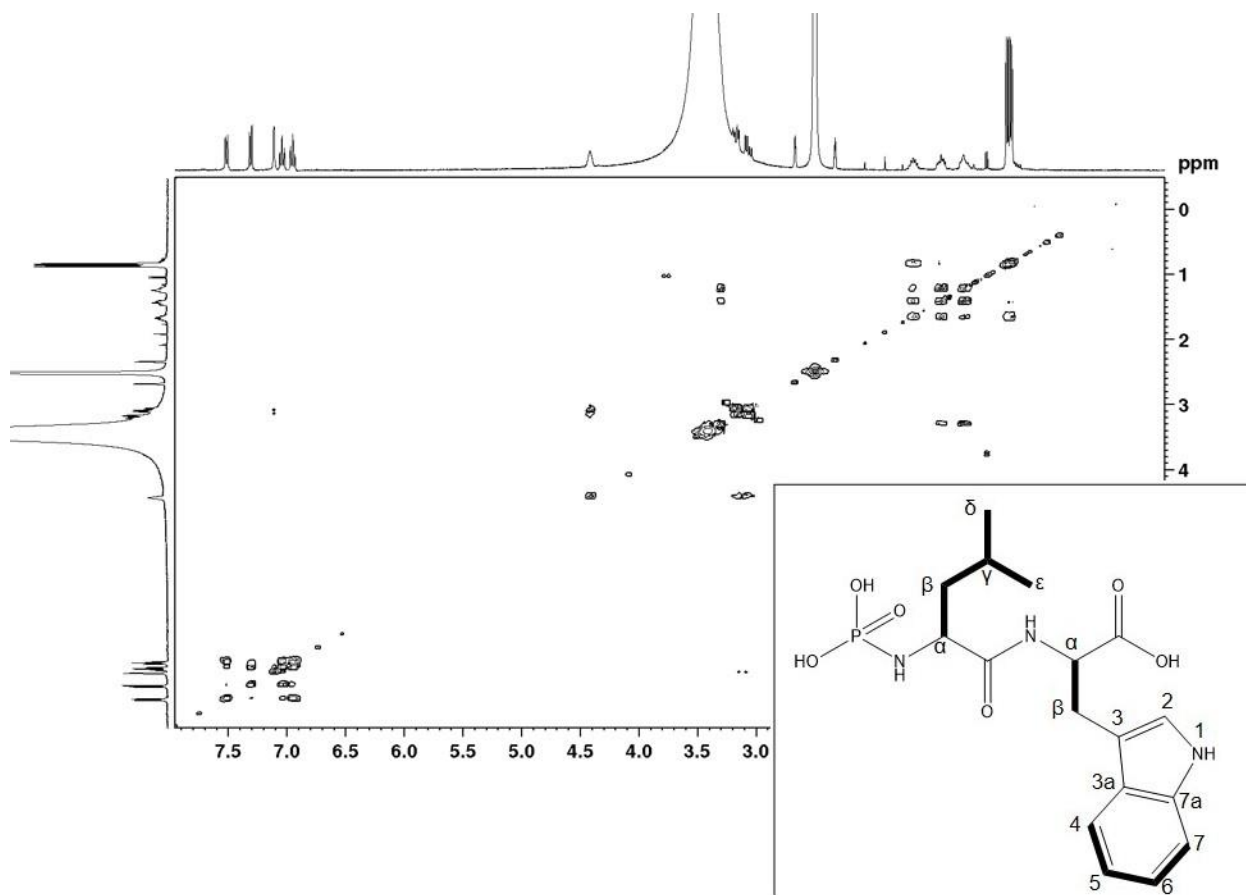


Figure S26: ^1H - ^1H COSY NMR spectrum of 5 in d_6 -DMSO (400 MHz).

Bold lines in the insert represent the observed ^1H - ^1H COSY correlations.

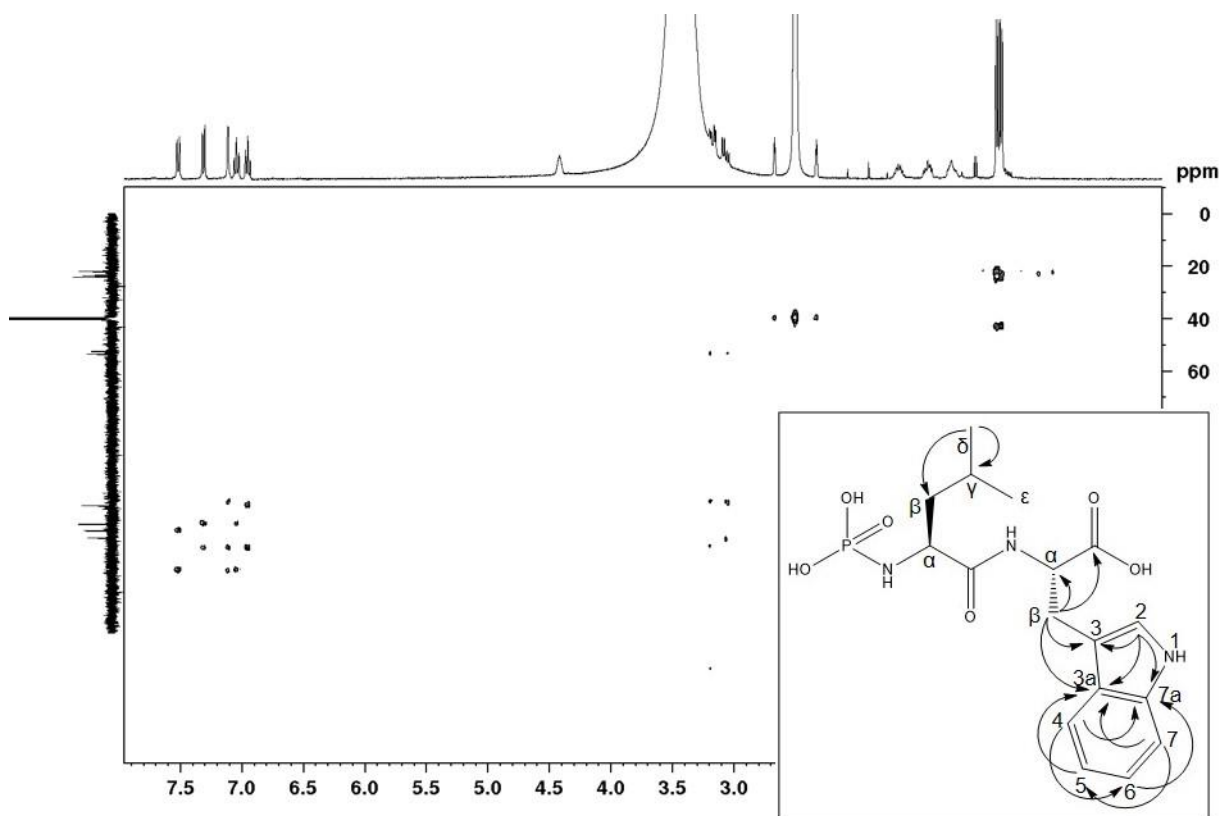


Figure S27: ^1H - ^{13}C HMBC NMR spectrum of 5 in d_6 -DMSO (400 MHz).

Arrows indicate key ^1H - ^{13}C HMBC long-range correlations.

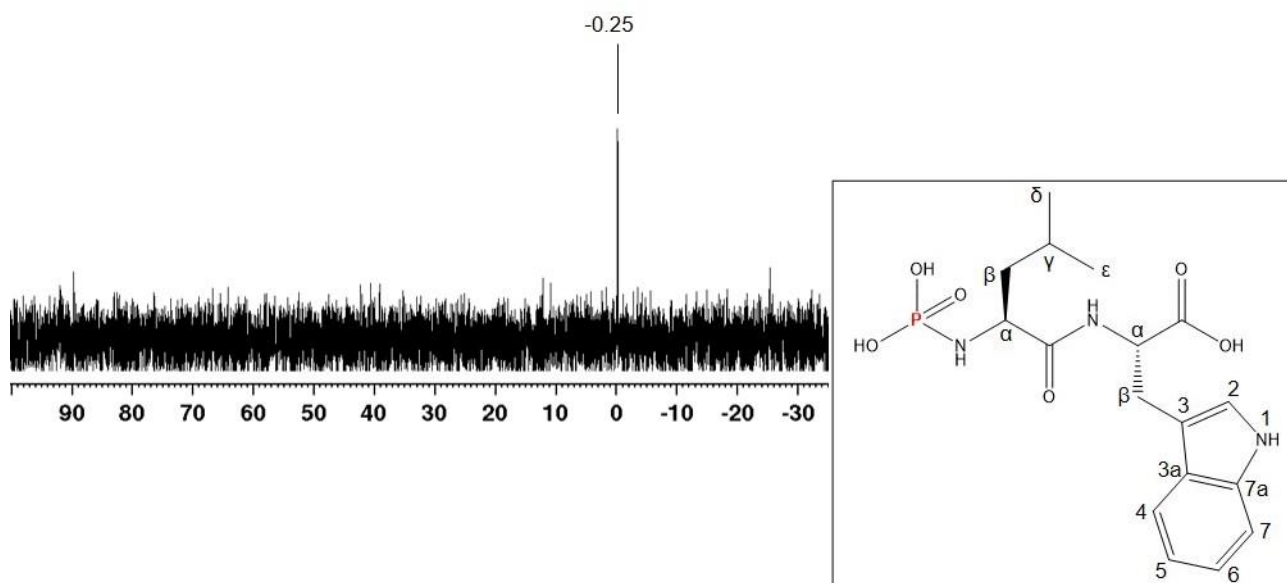


Figure S28: ^{31}P NMR spectrum of 5 in d_6 -DMSO (162 MHz).

The phosphate atom is marked in red.

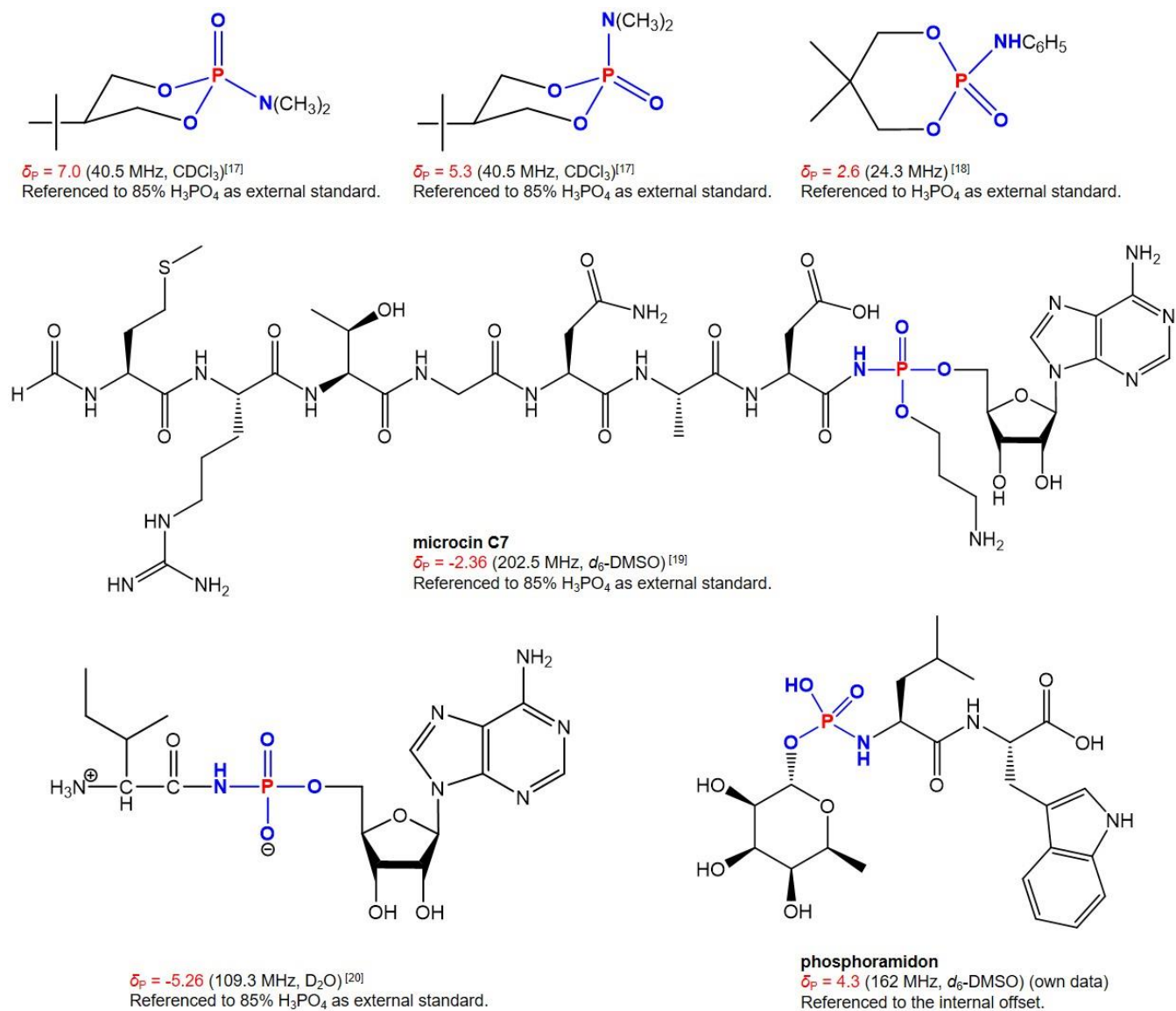


Figure S29: δ_P -reference values of selected phosphoramidate-containing natural products and synthetic compounds.

The corresponding δ_P value is indicated in red, while the phosphoramidate group is indicated in blue.¹⁷⁻²⁰

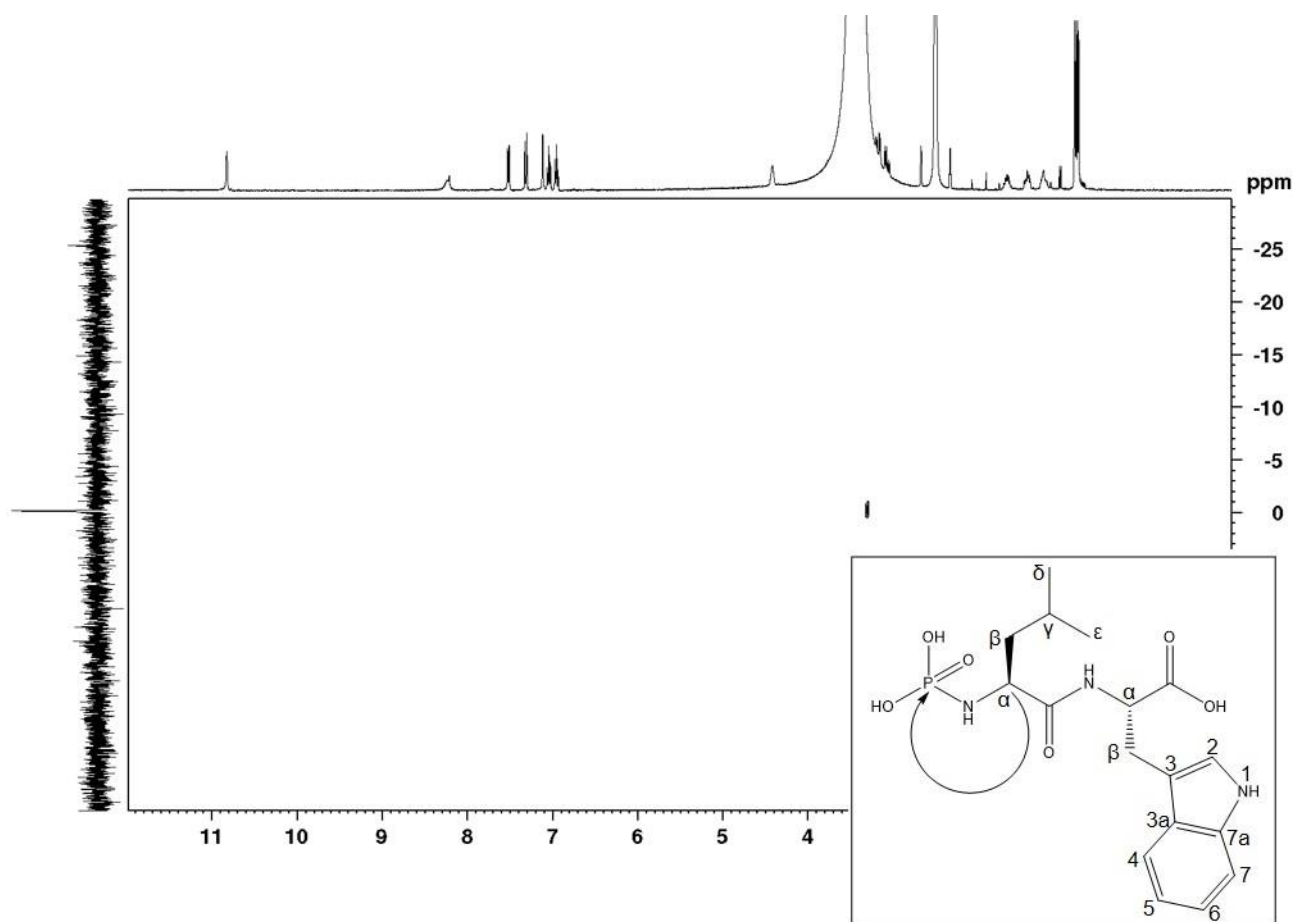


Figure S30: ^1H - ^{31}P HMBC NMR spectrum of 5 in d_6 -DMSO (400 MHz).

Arrow indicate ^1H - ^{31}P HMBC correlation.

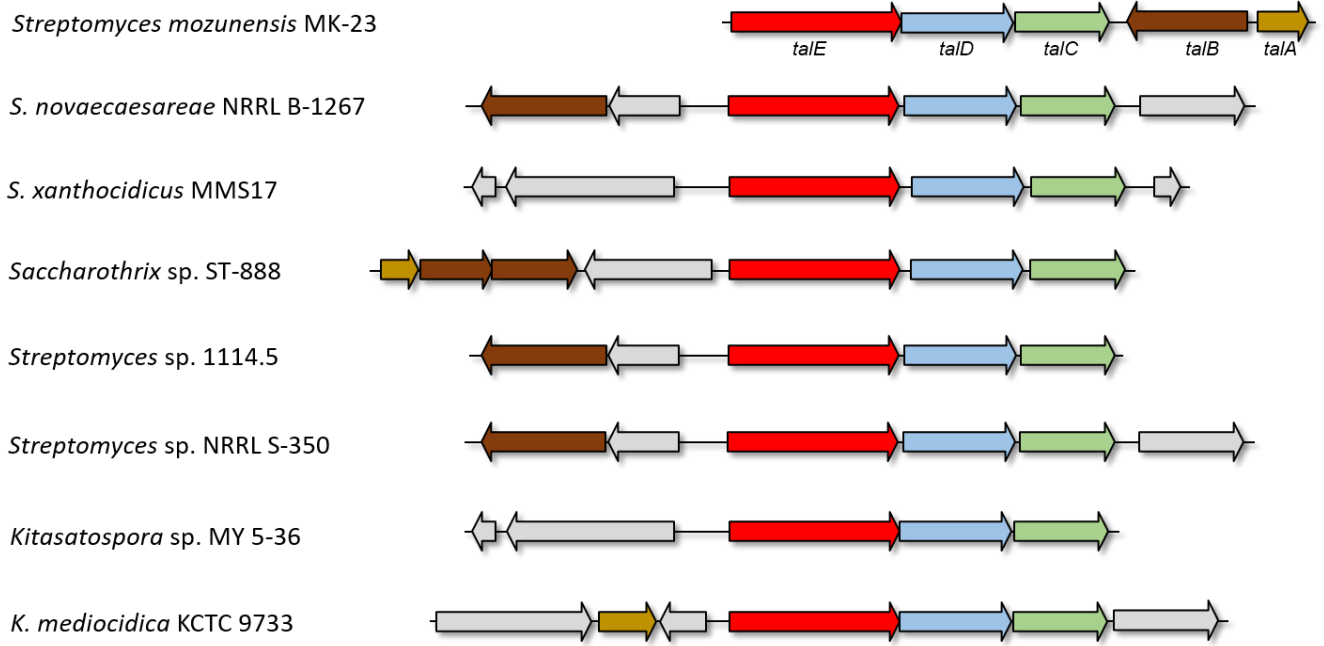


Figure S31: Homologous phosphoramidate pathways.

Selected orphan pathways containing a talCDE-like putative operon.

References

1. Sambrook, J.; Russell, D., *Molecular cloning. A Laboratory Manual*. 3era. ed. 1: 1.32-1.34. Cold Spring Harbour Lab Press, New York: 2001.
2. Kieser, T., *Prac Strept Gen*. John Innes Foundation: 2000.
3. Murao, S.; Katsura, M.; Fukuhara, K.-i.; Oda, K., New metallo proteinase inhibitor (MK-I) produced by *Streptomyces mozunensis* MK-23. *Agric Biol Chem* **1980**, *44* (3), 701-703.
4. Seemann, T., Prokka: rapid prokaryotic genome annotation. *Bioinform* **2014**, btu153.
5. Meyer, F.; Goesmann, A.; McHardy, A. C.; Bartels, D.; Bekel, T.; Clausen, J.; Kalinowski, J.; Linke, B.; Rupp, O.; Giegerich, R., GenDB—an open source genome annotation system for prokaryote genomes. *Nucl Ac Res* **2003**, *31* (8), 2187-2195.
6. Altschul, S. F.; Madden, T. L.; Schäffer, A. A.; Zhang, J.; Zhang, Z.; Miller, W.; Lipman, D. J., Gapped BLAST and PSI-BLAST: a new generation of protein database search programs. *Nucl Ac Res* **1997**, *25* (17), 3389-3402.
7. Medema, M. H.; Blin, K.; Cimermancic, P.; de Jager, V.; Zakrzewski, P.; Fischbach, M. A.; Weber, T.; Takano, E.; Breitling, R., antiSMASH: rapid identification, annotation and analysis of secondary metabolite biosynthesis gene clusters in bacterial and fungal genome sequences. *Nucl Ac Res* **2011**, *39* (suppl 2), W339-W346.
8. Medema, M. H.; Kottmann, R.; Yilmaz, P.; Cummings, M.; Biggins, J. B.; Blin, K.; de Bruijn, I.; Chooi, Y. H.; Claesen, J.; Coates, R. C.; Cruz-Morales, P.; Duddela, S.; Dusterhus, S.; Edwards, D. J.; Fewer, D. P.; Garg, N.; Geiger, C.; Gomez-Escribano, J. P.; Greule, A.; Hadjithomas, M.; Haines, A. S.; Helfrich, E. J.; Hillwig, M. L.; Ishida, K.; Jones, A. C.; Jones, C. S.; Jungmann, K.; Kegler, C.; Kim, H. U.; Kotter, P.; Krug, D.; Masschelein, J.; Melnik, A. V.; Mantovani, S. M.; Monroe, E. A.; Moore, M.; Moss, N.; Nutzmann, H. W.; Pan, G.; Pati, A.; Petras, D.; Reen, F. J.; Rosconi, F.; Rui, Z.; Tian, Z.; Tobias, N. J.; Tsunematsu, Y.; Wiemann, P.; Wyckoff, E.; Yan, X.; Yim, G.; Yu, F.; Xie, Y.; Aigle, B.; Apel, A. K.; Balibar, C. J.; Balskus, E. P.; Barona-Gomez, F.; Bechthold, A.; Bode, H. B.; Borriss, R.; Brady, S. F.; Brakhage, A. A.; Caffrey, P.; Cheng, Y. Q.; Clardy, J.; Cox, R. J.; De Mot, R.; Donadio, S.; Donia, M. S.; van der Donk, W. A.; Dorrestein, P. C.; Doyle, S.; Driessen, A. J.; Ehling-Schulz, M.; Entian, K. D.; Fischbach, M. A.; Gerwick, L.; Gerwick, W. H.; Gross, H.; Gust, B.; Hertweck, C.; Hofte, M.; Jensen, S. E.; Ju, J.; Katz, L.; Kaysser, L.; Klassen, J. L.; Keller, N. P.; Kormanec, J.; Kuipers, O. P.; Kuzuyama, T.; Kyrpides, N. C.; Kwon, H. J.; Lautru, S.; Lavigne, R.; Lee, C. Y.; Linqun, B.; Liu, X.; Liu, W.; Luzhetskyy, A.; Mahmud, T.; Mast, Y.; Mendez, C.; Metsa-Ketela, M.; Micklefield, J.; Mitchell, D. A.; Moore, B. S.; Moreira, L. M.; Muller, R.; Neilan, B. A.; Nett, M.; Nielsen, J.; O'Gara, F.; Oikawa, H.; Osbourn, A.; Osburne, M. S.; Ostash, B.; Payne, S. M.; Pernodet, J. L.; Petricek, M.; Piel, J.; Ploux, O.; Raaijmakers, J. M.; Salas, J. A.; Schmitt, E. K.; Scott, B.; Seipke, R. F.; Shen, B.; Sherman, D. H.; Sivonen, K.; Smanski, M. J.; Sosio, M.; Stegmann, E.; Sussmuth, R. D.; Tahlan, K.; Thomas, C. M.; Tang, Y.; Truman, A. W.; Viaud, M.; Walton, J. D.; Walsh, C. T.; Weber, T.; van Wezel, G. P.; Wilkinson, B.; Willey, J. M.; Wohlleben, W.; Wright, G. D.; Ziemert, N.; Zhang, C.; Zotchev, S. B.; Breitling, R.; Takano, E.; Glockner, F. O., Minimum Information about a Biosynthetic Gene cluster. *Nat Chem Biol* **2015**, *11* (9), 625-31.
9. Schorn, M.; Zettler, J.; Noel, J. P.; Dorrestein, P. C.; Moore, B. S.; Kaysser, L., Genetic Basis for the Biosynthesis of the Pharmaceutically Important Class of Epoxyketone Proteasome Inhibitors. *ACS Chem Biol* **2014**, *9* (1), 301-309.
10. Kaysser, L.; Bernhardt, P.; Nam, S.-J.; Loesgen, S.; Ruby, J. G.; Skewes-Cox, P.; Jensen, P. R.; Fenical, W.; Moore, B. S., Merochlorins A–D, Cyclic Meroterpenoid Antibiotics Biosynthesized in Divergent Pathways with Vanadium-Dependent Chloroperoxidases. *J Am Chem Soc* **2012**, *134* (29), 11988-11991.
11. MacNeil, D. J.; Gewain, K. M.; Ruby, C. L.; Dezeny, G.; Gibbons, P. H.; MacNeil, T., Analysis of *Streptomyces avermitilis* genes required for avermectin biosynthesis utilizing a novel integration vector. *Gene* **1992**, *111* (1), 61-68.
12. Flett, F.; Mersinias, V.; Smith, C. P., High efficiency intergeneric conjugal transfer of plasmid DNA from *Escherichia coli* to methyl DNA-restricting streptomycetes. **1997**, *155* (2), 223-229.
13. Gust, B.; Challis, G. L.; Fowler, K.; Kieser, T.; Chater, K. F., PCR-targeted *Streptomyces* gene replacement identifies a protein domain needed for biosynthesis of the sesquiterpene soil odor geosmin. *Proc Natl Acad Sci* **2003**, *100* (4), 1541-1546.
14. Datsenko, K. A.; Wanner, B. L., One-step inactivation of chromosomal genes in *Escherichia coli* K-12 using PCR products. *Proc Natl Acad Sci U S A* **2000**, *97* (12), 6640-5.
15. Rose, M. E.; Prescott, M. C.; Wilby, A. H.; Galpin, I. J., Analysis of peptides with unusual structural features by fast atom bombardment mass spectrometry: Protease inhibitors. **1984**, *11* (1), 10-23.
16. Wolf, S.; Schmidt, S.; Müller-Hannemann, M.; Neumann, S. J. B. B., In silico fragmentation for computer assisted identification of metabolite mass spectra. **2010**, *11* (1), 148.
17. Bentrude, W. G.; Tan, H.-W., Conformations of saturated cyclic phosphorus heterocycles. II. 5-tert-Butyl-2-amino-1,3,2-dioxaphosphorinanes. Apparent effects of phosphorus-nitrogen vicinal interactions on the conformational energy of amino groups on trivalent phosphorus and the influence of lone pair orientation on 3FHeqP. *J Am Chem Soc* **1973**, *95* (14), 4666-4675.
18. Stec, W. J.; Okruszek, A.; Lesiak, K.; Uznanski, B.; Michalski, J., New synthesis of S(Se)-alkyl phosphorothio(seleno)lates from the corresponding phosphoroanilidates. Stereospecific cleavage of the phosphorus-nitrogen bond in chiral phosphoroanilidates. *J Org Chem* **1976**, *41* (2), 227-233.
19. González-Pastor, J. E.; San Millán, J. L.; Castilla, M. A.; Moreno, F., Structure and organization of plasmid genes required to produce the translation inhibitor microcin C7. **1995**, *177* (24), 7131-7140.
20. Moriguchi, T.; Yanagi, T.; Kunimori, M.; Wada, T.; Sekine, M., Synthesis and Properties of Aminoacylamido-AMP: Chemical Optimization for the Construction of an N-Acyl Phosphoramidate Linkage. *J Org Chem* **2000**, *65* (24), 8229-8238.